Journal of Atherosclerosis and Thrombosis Vol. 13, No. 1

Original Article

The Lipoprotein Fraction between VLDL and LDL Detected by Biphasic Agarose Gel Electrophoresis Reflects Serum Remnant Lipoprotein and Lp(a) Concentrations

Itsuko Sato[1], Takahiro Taniguchi[2], Yuichi Ishikawa[3], Mari Kusuki[1], Fujio Hayashi[1], Masahiko Mukai[1], Seiji Kawano[1,6], Shinichi Kondo[4], Shizuya Yamashita[5], and Shunichi Kumagai[1,6]

[1] *Clinical Laboratory, Kobe University Hospital, Kobe, Japan.*
[2] *Division of Cardiovascular and Respiratory Medicine, Department of Internal Medicine, Kobe University Graduate School of Medicine, Kobe, Japan.*
[3] *Faculty of Health Sciences, Kobe University School of Medicine, Kobe, Japan.*
[4] *Department of Internal Medicine, Kakogawa Municipal, Hospital, Hyogo, Japan.*
[5] *Department of Internal Medicine and Molecular Science, Osaka University Graduate School of Medicine, Osaka, Japan.*
[6] *Department of Clinical Pathology and Immunology, Kobe University Graduate School of Medicine, Kobe, Japan.*

We analyzed lipoprotein profiles in 616 Japanese by biphasic agarose gel electrophoresis using Chol/Trig Combo™ to yield HDL, VLDL, LDL and CM fractions which were stained with cholesterol and triglyceride reagents, respectively. To further evalute the pattern of electrophoresis, we analyzed the fraction between VLDL and LDL to confirm the possibility of a MidBand by using an automatic-five-fraction function. The cholesterol concentrations in MidBand (MidBand-C) showed a good correlation to remnant-like particle-cholesterol (RLP-C) (r = 0.95) in 23 consecutive samples (TC < 220 mg/dl, Lp(a) < 30 mg/dl). However, MidBand-C concentrations of subjects with high Lp(a) levels (Lp(a) > 30 mg/dl) were also high compared to RLP-C concentrations. The average MidBand-C levels in elderly normolipidemic control subjects (TC < 220, TG < 150) were 5.2 ± 2.4 mg/dl in 30 males (mean age, 70 ± 10 years) and 5.4 ± 2.0 mg/dl in 40 females (64 ± 11 years). The average MidBand-C levels of normolipidemic patients with coronary artery diseases (CAD; TC < 220, TG < 150) were 9.4 ± 4.1 mg/dl in 126 males (mean age, 66 ± 10 years) and 9.1 ± 4.0 mg/dl in 44 females (67 ± 10 years). These levels were significantly higher than control values (p < 0.0001). Areas under ROC curves were greater for MidBand-C than for TC, LDL-C and TG when used to discriminate between the patients with CAD and normolipidemic control subjects for each sex. There results suggest that the MidBand-C level may be useful as an indicator of risk for CAD. *J Atheroscler Thromb, 2006; 13: 55–61.*

Key words: Agarose gel electrophoresis, Automatic five-fraction, Remnant like particles-cholesterol, Coronary artery disease.

Introduction

The major remnant lipoproteins are a mixture of the exogenous chylomicron remnant derived from the intestine and the endogenous very low density lipoprotein (VLDL) remnant (IDL) derived from the liver. Methods have been developed to measure remnant lipoproteins. Remnant lipoproteins have been identified as atherogenic (1).

Address for correspondence: Itsuko Sato, Clinical Laboratory, Kobe University Hospital, 7-5-2, Kusunoki-cho, Chuo-ku, Kobe 650-0017, Japan.
E-mail: itsuko@med.kobe-u.ac.jp
Received January 28, 2004
Accepted for publication November 7, 2005

We reported that serum levels of remnant-like particle cholesterol (RLP-C) were increased in patients with diabetes and impaired glucose tolerance (2). We also reported that remnant lipoproteins had unique biological effects such as the induction of apotosis of cultured endothelial cells (3). VLDL remnants can be separated by the ultracentrifugal method at a density of 1.006–1.019 g/ml (4). However, this method is not suitable for routine analysis, because it takes hours, and the processing of multiple specimens is difficult (5).

Agarose gel electrophoresis is an authentic method of detecting remnant lipoprotein which appears as a broad band. The mid-band in polyacrylamide gel electrophoresis is also well known as the band of remnant lipoprotein (4). However, these methods are qualitative not quantitative. Recently a quantitative assay for RLP-C has been developed (6), and an elevation of plasma RLP-C levels was reported in patients with coronary artery diseases (CAD) (7). But there are considerable numbers of patients with type I and V hyperlipidemia whose levels of RLP-C appear abnormal in immunoadsorption assays with antibody. Therefore, it is important to develop simple and comprehensive methods to measure remnant lipoprotein levels.

We analyzed the lipoprotein fractions by using the agarose gel electrophoresis with Chol/Trig Combo™, which can quantify each lipoprotein fraction on the basis of the separate staining of cholesterol and TG and by automatic analysis. Based on this method, it is possible not only to measure the levels of HDL- cholesterol (HDL-C) and LDL-cholesterol (LDL-C) quantitatively, but also to recognize the entire pattern of lipoprotein fractions (8–11). We identified the fraction between the VLDL and LDL fractions using the Automatic five-fraction function of Chol/Trig Combo™ and elucidated that this fraction was closely related to the levels of RLP-C and increased in CAD patients compared with normolipidemic subjects. We named this fraction MidBand and clarified it's clinical significance.

Methods

Study subjects

We measured RLP-C and Lp(a) concentrations in 64 patients [31 males (mean age 60 ± 11 years, age range 31–81 years) and 33 females (63 ± 16, 26–80 years)], who requested a RLP-C test between 2000.03 and 2003.03.

The elderly control subjects were the 80 normolipidemic (TC 114–219 mg/dl, TG < 150 mg/dl) staff members of the Kobe University hospital enrolled in an annual medical checkup and patients 60 years or older who were free from CAD, liver disease, kidney disease and diabetes mellitus who were selected from among patients at Kobe University Hospital. These were 35 males (mean age 66 ± 13years, age range 41–90 years) and 45 females (64 ± 12, 50–88 years)

To evaluate the clinical usefullness of MidBand-C in CAD, 168 patients with CAD (TC 80–219 mg/dl, TG < 150 mg/dl) were admitted to Kobe University hospital and their diagnosis was confirmed by coronary angiography. This group consisted of 125 males (mean age 67 ± 10 years, age range 35–88 years) and 43 females (68 ± 9, 47–83 years).

Hospital staff were ordered with informed consent to come to blood sampling in the fasting state. Sera from the patients with CAD were drawn in a 12-hour fasted state with venopuncture. These samples were made anonymous without linking.

Biochemical analysis

Serum total cholesterol (TC) and TG concentrations were measured using an auto analyzer TBA-80M (TOSHIBA, Tokyo, Japan) by the enzymatic method. The RLP-C concentration was measured by the immune adsorption method (JIMROII, Japan). The serum Lp(a) concentration was measured using an auto analyzer TBA-80FR (TOSHIBA) by the latex agglutination immunoassay.

Agarose gel electrophoreisis analysis

The serum samples were subjected to the lipoprotein analysis using agarose gel electrophoresis (Rapid Electrophoresis, Helena Laboratories, Beaumont, Texas) and the gels were stained with cholesterol and TG reagent. The conditions for electrophoresis were as follows; serum application volume was 1μ, and electrophoresis time was 18 min at 400 volts, and 20°C. Elution profiles were analyzed by an automatic densitometer, Chol/Trig Combo™ (Helena Kennkyusyo, Saitama, Japan).

Apolipoprotein B48 (apoB48) and Apolipoproteon B100 (B100) were identified with immunoblotting on the nitrocellulose film where the agarose gels were transferred. For detecting apo B48 and apo B100, we used anti-apoB48-151 monoclonal antibody (Fujirebio Co, Tokyo, Japan) and anti-apo B100 monoclonal antibody (Biochemical Division, Ohio), respectively. Ofuto® cream (Milk fat 35%, 547 kcal. Jyoumou Shokuhin company, Gunma, Japan) was used in the fat load. The samples which could not be measured on the day were stored at –40°C with the addition 1/20 (vol/vol) of dimethyl sulfoxide (8). This preservation method was effective up to four weeks (data not shown).

Statistical analysis

Data are expressed as the mean ± SD. Pearson's Correlation coefficient was used for the relationship between MidBand-C and RLP-C. Differences were examined with Student's *t* test. The computer analysis was done using Stat View Ver. 5.0. A *p*-value less than 0.01 was considered statistically significant. Receiver-operative charac-

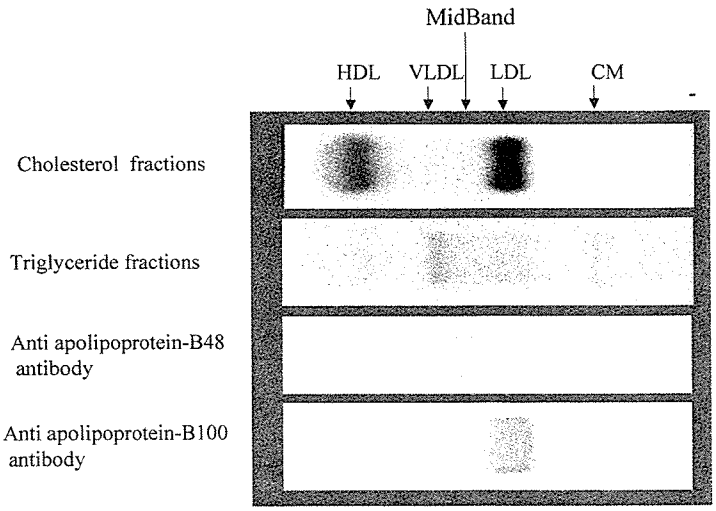

Fig. 1. Electrophoregram of cholesterol fractions, triglyceride fractions, apo B48 or apo B100. Apo B48 and apo B100 were detected by immunoblotting with anti -apo B48 or anti-apo B100 antibody. Sera were electrophoresed 4 hours after fat load (Ofuto™)

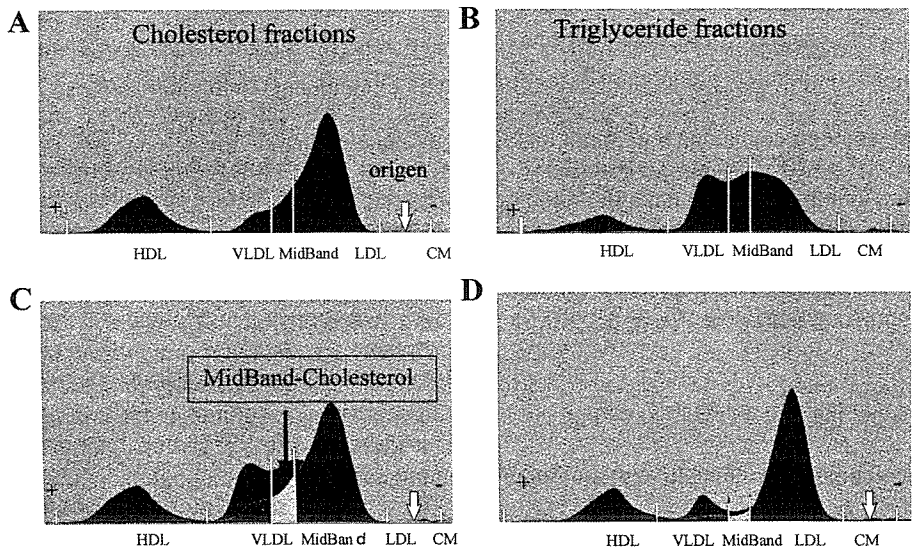

Fig. 2. The representative densitometric scanning patterns for Chol/Trig Combo™.
(A): cholesterol stain (B): triglyceride stain (C): layer in A and B (D): an example of a normolipidemic control subject, TC 202, TG 86, HDL-C 65, Mid Band-C 2.0, RLP-C < 2.5 (mg/dl)

teristics curve analysis was used to show performance figures. For the computation and analysis of ROC curves, we used the software program Med Calc, Ver. 6.01 (Med Calc Software).

Results

Determination of MidBand

We established automatic-five-fraction on the strength of the electric charge with apolipoprotein. The fraction eluted between the VLDL and LDL fractions in agarose gel electrophoresis of Chol/Trig Combo™ was defined as MidBand.

To confirm whether MidBand was rich in apoB48, serum was selected 4 hours after the loading of fat (Ofuto™) and electrophoresed and transfered to a nitrocellulose membrane. Nitrocellulose membrane was immunoblotted with anti-human apoB48 antibody and compared with the electrophoregram of cholesterol fractions, TG fractions and fractions immunoblotted with anti apoB100 antibody. MidBand was rich in apoB48, and the LDL fraction was rich in apoB100 (Fig. 1).

For example, agarose gels were stained for cholesterol (Fig. 2A) or TG (Fig. 2B) after electrophoresis and analyzed by the automatic densitometer Chol/Trig Combo™. After both patterns were imposed as shown in Fig. 2C,

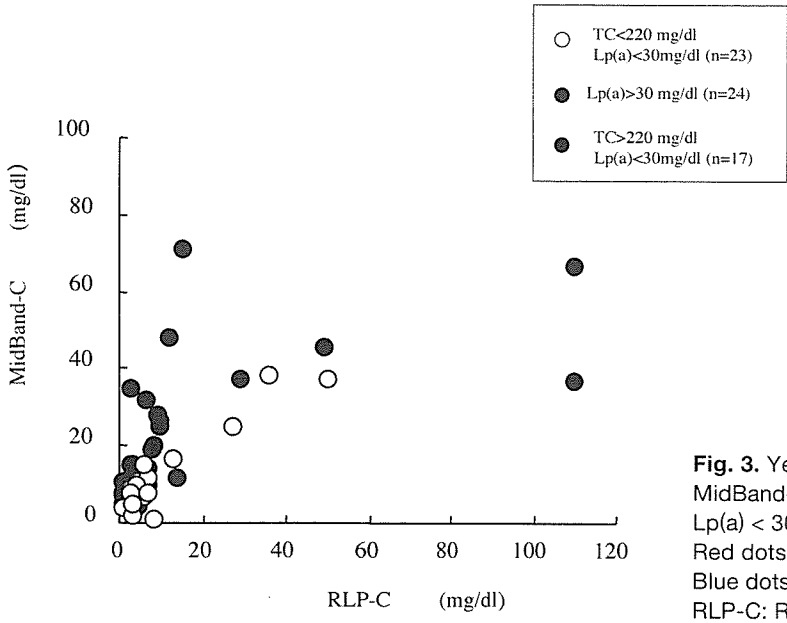

Fig. 3. Yellow dots: A significant positive correlation between MidBand-C levels and RLP-C levels when TC < 220 mg/dl and Lp(a) < 30 mg/dl.
Red dots: Lp > 30 mg/dl
Blue dots: TC > 220 mg/dl and Lp(a) < 30 mg/dl
RLP-C: Remnant-like particle cholesterol

MidBand was determined as the fraction between LDL and VLDL fractions. A representative profile of a normolipidemic subject is shown in Fig. 2D. The MidBand -cholesterol (MidBand-C) concentration was calculated from the serum cholesterol level and percentage of MidBand in the cholesterol fraction of the agarose gel electrophoretogram.

Relationship among MidBand-C, RLP-C and Lp(a)

To evaluate the relationship between MidBand-C and RLP-C, we measured RLP-C concentrations of 64 subjects and compared them to MidBand-C concentrations. We selected 23 subjects with both a TC of less than 220 mg/dl and Lp(a) concentration of less than 30 mg/dl out of the 64 subjects. As shown in Fig. 3 (yellow dot), there was a significant positive correlation between concentrations of MidBand-C and RLP-C in subjects with a correlation coefficient(r) of 0.95 ($p < 0.001$). However, MidBand-C concentrations of hyperlipidemic patients deviated from the standard line (Fig. 3, red dot and blue dot). MidBand-C concentrations of subjects with high Lp(a) levels were also high compared with RLP-C concentrations. As we have already reported, Lp(a) at levels of more than 30 mg/dl migrates as a peak of cholesterol between VLDL and LDL using this method (13). This position is the same as that of MidBand. Representative elution profiles are shown in Fig.4. In sample A, the Lp(a) concentration was 142 mg/dl showing a sharp MidBand-C peak. Sample B was from a type IIb hyperlipidemic patient and MidBand-C is the mid-band. Sample C was obtained from a type III hyperlipidemic patient and had a broad beta-band in the lipoprotein fraction. Sample D showed the presence of chylomicron and a high concentration of VLDL-TG, indicating type V hyperlipidemia.

Comparison of MidBand-C levels of normolipidemic subjects with patients with CAD

Table 1 shows a summary of the clinical characteristics of the elderly control subjects and the patients with CAD. Significant differences in HDL-C and MidBand-C concentrations were observed between the two groups in each sex.

To elucidate the clinical significance of MidBand-C in CAD, we measured the MidBand-C concentrations of the patients with CAD. Mean MidBand-C concentrations were 9.4 ± 4.1 and 9.2 ± 4.0 mg/dl in the male and female patients, and significantly higher than in control subjects ($p > 0.0001$) (Fig. 5).

A ROC analysis was performed for MidBand-C, HDL-C, LDL-C, TC and TG in the CAD patients and control subjects in males (Fig.6) and females (Fig.7). The area under the ROC curve (AUC) for MidBand-C in males and females was 0.80 and 0.79, respectively, showing a significant difference from that for LDL-C, TC and TG. ROC curves of HDL-C and MidBand-C almost overlapped and there was no significant difference.

Discussion

In the present study, we demonstrated that MidBand-C concentrations analyzed by agarose gel electrophoresis and automatic densitometer showed a significant correlation with RLP-C concentrations. MidBand is consid-

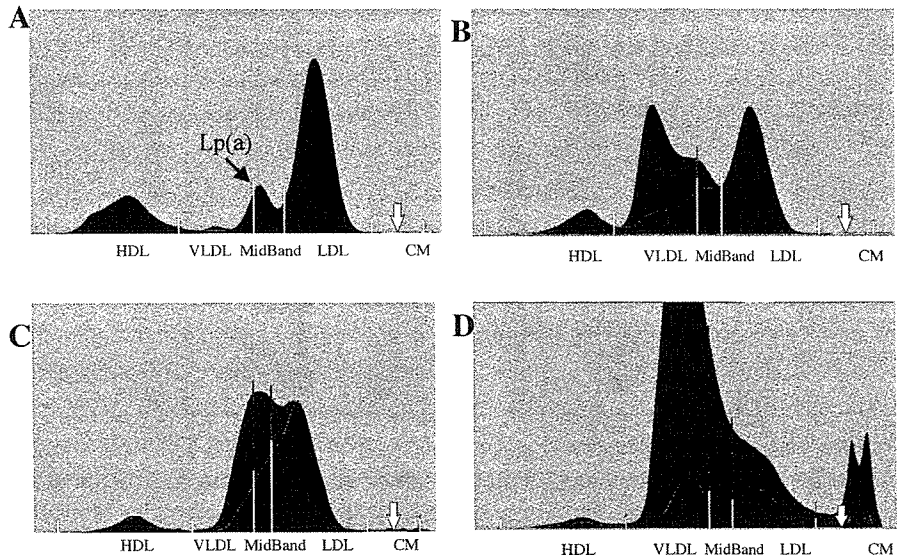

Fig. 4. Densitometric scanning patterns of hyperlipidemia.
Patient A had type IIa hyperlipidemia, and the mid-band; TC 311, TG 41, RLP-C 2.9, MidBand-C 39.5, Lp(a) 142 mg/dl. Patient B had type IIb hyperlipidemia, and the mid-band; TC 252, TG 264, RLP-C 9.0, MidBand-C 46.4 mg/dl. Patient C had type III hyperlipidemia, and a broad beta-band in the lipoprotein fraction; TC 232, TG 342,RLP-C 12.0, MidBand-C 58.0 mg/dl. Patients D had the type V hyperlipidemia, and an increase of chiromicron; TC 167, TG967, RLP-C 71.0, MidBand-C 14.0 mg/dl.

Table 1. Clinical characteristics of CAD patients and elderly control subjects

	Men		Female	
	control ($n = 35$)	CAD ($n = 125$)	control ($n = 45$)	CAD ($n = 43$)
Age (year)	66.1 ± 12.6	66.7 ± 9.6	63.7 ± 11.5	68.1 ± 9.3
TC (mg/dl)	164.7 ± 30.7	169.3 ± 29.7	178.7 ± 22.3	173.3 ± 24.5
TG (mg/dl)	86.0 ± 28.8	92.2 ± 30.7	92.0 ± 23.4	98.5 ± 28.3
LDL-C (mg/dl)	104.7 ± 24.2	103.9 ± 26.4	92.1 ± 20.8	104.5 ± 22.5
HDL-C (mg/dl)	61.3 ± 14.4	42.4 ± 13.3*	69.4 ± 17.5	47.4 ± 13.9**
MidBand-C (mg/dl)	5.2 ± 2.3	9.4 ± 4.1*	5.5 ± 2.0	9.2 ± 3.9**

* Significantly different from the value of control men, $p < 0.0001$
** Significantly different from the value of control female, $p < 0.0001$

ered similar to the mid-band observed in polyacrylamide gel electrophoresis (PAGE). However, it is not possible to conduct a quantitative analysis of remnant lipoproteins by PAGE. Additionally, preparative and analytical ultracentrifugation methods have been used to separate VLDL and IDL. However these methods are labor-intensive and complex. With our method using Chol/Trig Combo™, the operation is simple and semi-automated. Moreover, one is able not only to recognize the entire lipoprotein profile but also to quantitate the cholesterol and TG of MidBand that is equivalent to the IDL or remnant lipoprotein. We demonstrated that the MidBand richly contained apo B48.

To investigate the relation between MidBand-C and RLP-C, we measured RLP-C concentrations of 23 subjects with both a TC concentration of less than 220 mg/dl and a Lp(a) concentation of less than 30 mg/dl. In these subjects, there was a significant correlation between RLP-C and MidBand-C. Moreover, Lp(a) at levels of more than 30 mg/dl migrates as the same peak as MidBand-C. These results suggested that MidBand-C reflected VLDL remnants and Lp(a). Both are known to be atherogenic.

We analyzed MidBand-C in 80 elderly control subjects. To investigate the significance of the MidBand-C con-

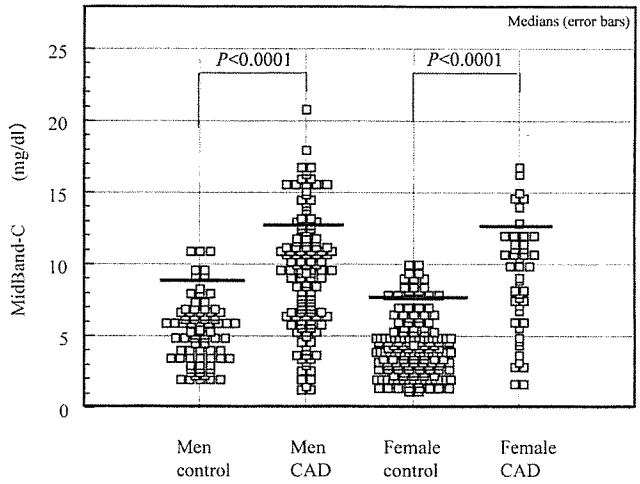

Fig. 5. Levels of MidBand-C in the elderly normolipidemic control subjects and the normolipidemic patients with CAD. There was a significant difference in MidBand-C levels between the control and CAD in each sex.

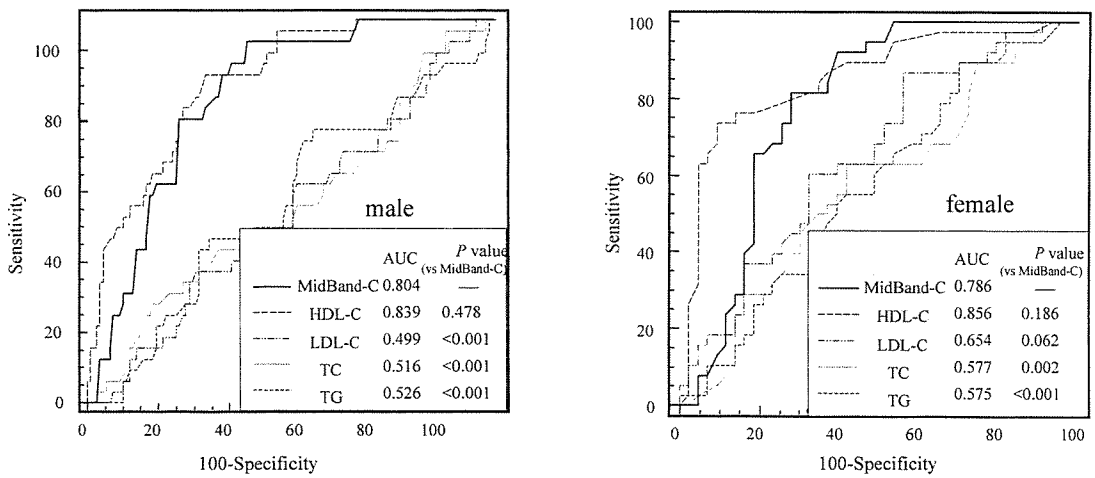

Fig. 6. and Fig. 7. Receiver operating characteristic curves of MidBand-C, HDL-C, LDL-C, TC and TG when used to discriminate between the patients with CAD and control subjects in males and females. AUC: Area under the curve.

centration in CAD, we measured levels in 168 patients with CAD. Mean MidBand-C levels of CAD patients (9.4 ± 4.1 mg/dl and 9.2 ± 3.9 mg/dl in males and females, respectively) were significantly higher than those of elderly control subjects (5.2 ± 2.3 mg/dl and 5.5 ± 2.0 mg/dl, $p < 0.0001$). In the ROC analysis performed on CAD patients and control subjects, the AUC for MidBand-C was 0.80 for males and 0.79 for females. In addition, the AUC of MidBand-C was significantly higher than that for LDL-C, TC or TG, suggesting that the elevation in the concentration of MidBand-C could be a useful marker of the risk of developing CAD.

Considering these results, measurements of MidBand-C made using Chol/Trig Combo™ may be important to evaluate the risk of CAD.

Conclusion

We defined MidBand as the fraction between LDL and the VLDL fractions in Chol/Trig Combo™. MidBand-C reflected the serum levels of RLP-C and Lp(a), and may be an important index with which to estimate the risk of CAD.

References

(1) Havel RJ: Postprandical hyperlipidemia and remnant lipoproteins. Curr Opin Lipidol, 5: 102–109, 1994

(2) Watanabe N, Taniguchi T, Taketoh H, Kitagawa Y, Namura H, Yoneda N, Kurimoto Y, Yamada S, and Ishikawa Y: Elevated Remnant-like lipoprotein particles in impaired glucose tolerance and type 2 diabetic patients. Diabetes care, 22: 152–156, 1999

(3) Kawasaki S,Taniguchi T, Fujioka Y, Takahashi A, Takahashi T, Domoto K, Taguchi M, Ishikawa Y, and Yokoyama M: Chylomicron remnant induces apoptosis in vascular endothelial cells. Ann NY Acad Sci, 902: 336–341, 2000

(4) Nozaki S, Yamashita S, and Matsuzawa Y: Accumulation of Remnant Lipoprotein- Evalution and Its Mechanism. Atherosclerosis, 26: 279–282, 1999

(5) Takeuchi N and Saheki Y: Evaluation and Problems of Ultracentrifugel Techniqal for Separation and Analysis of Serum Lipoprotein. Comparison with Other Analytical Methods. Jpn J Pahol, 41: 750–758, 1993

(6) Akuzawa K, Nakano T, Sekiuchi I, Shimoyama M, Adachi M, Tange S, Tanaka A, Tada N, and Nakajima K: Remnant-like Particls-cholesterol (RLP-C) Assay and its Clinical Application to Lipid Tests in a Postprandial as well as Fasting State. Jpn J Pathol, 43: 1159–1167, 1995

(7) Leary ET, Wang T, and Baker DJ: Evolution of an immunoseparation method for quantitative measurement of remnant-like particle-cholesterol in serum and plasma. Clin Chem, 448: 2490–2498, 1998

(8) Kido T, Kurata H, Iwamoto T, Utsunomiya K, Matsumoto A, Tajima N, Itakura H, and Kondo K: Clinical application of apolipoprotein analysis by agarose gel electrophoresis. The Lipid, 9: 487–494, 1998

(9) Tsukamoto H, Hukada H, Ootake T, Kikuchi H, and Watanabe K: Evaluation of New Computer System for Analysis of Serum Lipoprotein Electrophoresis; Comparison with Ultracentrifugal Analysis. JJCLA, 25: 723–729, 2000

(10) Tanaka M, Inada Y, and Yoshino G: Detection of modified lipoproteins employing specific antibodies against apolipoproteins by Chol/Trig Combo™ and its clinical application. Jpn J Med Pharm Sci, 50: 551–556, 2003

(11) Muraoka K, Kiyohara Y, Kikuchi M, Tagawa N, Maeda A, and Kobayashi Y: Pathological Analysis of Hyperlipidemia by a Newly Developed Agrose Electrophoreses. Rinsho Kagaku, 31: 266–274, 2002 (Japanese)

(12) Nakazato I, Hisamura A, Morishima S, Furuta K, and Nishio H: On saving method of the serum sample for the lipid electrophoresis. Sample kenkyukai, 15: 35, 2001 (Japanese)

(13) Hyakuta M, Sato I, Hayasi F, Mukai M, Kondo S, and Kumagai S: Reason of Lp(a) Not Appearing as a Mid-band with the Chol/Trig Combo. JJCLA, 28: 52–58, 2003 (Japanese)

EXTENDED REPORT

Efficacy of rituximab (anti-CD20) for refractory systemic lupus erythaematosus involving the central nervous system

Mikiko Tokunaga, Kazuyoshi Saito, Daisuke Kawabata, Yoshitaka Imura, Takao Fujii, Shingo Nakayamada, Shizuyo Tsujimura, Masao Nawata, Shigeru Iwata, Taeko Azuma, Tsuneyo Mimori, Yoshiya Tanaka

Ann Rheum Dis 2007;**000**:1–7. doi: 10.1136/ard.2006.057885

See end of article for authors' affiliations

Correspondence to: Dr Y Tanaka, The First Department of Internal Medicine, School of Medicine, University of Occupational and Environmental Health, Japan, 1-1 Iseigaoka Yahata-nishi, Kitakyushu 807-8555 Japan; tanaka@med.uoeh-u.ac.jp

Accepted 30 October 2006
Published Online First 9 November 2006

Aim: Neuropsychiatric systemic lupus erythaematosus (NPSLE) is a serious treatment-resistant phenotype of systemic lupus erythaematosus. A standard treatment for NPSLE is not available. This report describes the clinical and laboratory tests of 10 patients with NPSLE before and after rituximab treatment, including changes in lymphocyte phenotypes.

Methods: Rituximab was administered at different doses in 10 patients with refractory NPSLE, despite intensive treatment.

Results: Treatment with rituximab resulted in rapid improvement of central nervous system-related manifestations, particularly acute confusional state. Rituximab also improved cognitive dysfunction, psychosis and seizure, and reduced the SLE Disease Activity Index Score at day 28 in all 10 patients. These effects lasted for >1 year in five patients. Flow cytometric analysis showed that rituximab down regulated CD40 and CD80 on B cells and CD40L, CD69 and inducible costimulator on CD4+ T cells.

Conclusions: Rituximab rapidly improved refractory NPSLE, as evident by resolution of various clinical signs and symptoms and improvement of radiographic findings. The down regulation of functional molecules on B and T cells suggests that rituximab modulates the interaction of activated B and T cells through costimulatory molecules. These results warrant further analysis of rituximab as treatment for NPSLE.

Systemic lupus erythaematosus (SLE) is an autoimmune disease characterised by multiple lesions induced by activation of autoreactive T cells and overproduction of autoantibodies by B cells. The involvement of the central nervous system (CNS) in SLE is often intractable, complicating the course of the disease in about 12–75% of patients with SLE. The involvement of the CNS has a negative clinical impact with a 5-year survival of 55–85% and is associated with poor prognosis.[1 2] Neuropsychiatric systemic lupus erythaematosus (NPSLE) exhibits a wide range of symptoms unrelated to SLE activation, which include organic and mental disorders, often associated with impairment of consciousness and/or convulsions. These organic disorders may become permanent, eventually leading to long-term or irreversible decline in higher mental functions.

CNS immune abnormalities have an important role in such disease states. Therefore, a trial of intensive treatment, including the combination of potent immunosuppressive treatment and plasma exchange (PE), depending on the disease type and its severity, may be advisable in an effort to control autoreactive lymphocytes.[3–10] Although the severity of NPSLE correlates with prognosis, there is no established treatment protocol and many cases are resistant to treatment making this condition difficult to control.

This study describes the results of treatment of patients with NPSLE who had previously failed to respond to various immunosuppressants. Our approach was based mainly on the use of anti-CD20 antibody (rituximab), a chimeric antibody that directly targets B cells.[11 12] Rituximab is a biological preparation that eliminates B cells through a variety of mechanisms such as antibody-dependent cellular cytotoxicity, complement-dependent cytotoxicity and apoptosis. Rituximab has recently been used for the treatment of a variety of SLE disease conditions and good therapeutic response has been reported.[13–16] We investigated the short-term and long-term responses to rituximab treatment in 10 patients with NPSLE, and report that some showed marked improvement following rituximab treatment. Moreover, the results showed that rituximab modulated the functional molecules of activated lymphocytes, implying the efficacy of anti-CD20 antibody treatment for CNS lesions in patients with SLE, otherwise resistant to other treatments.

MATERIALS AND METHODS

Patients

The study subjects were 10 patients who had been previously diagnosed with SLE based on the American College of Rheumatology criteria.[17] The inclusion criteria were (1) the presence of a highly active disease and (2) CNS lesions resistant to conventional treatment. None of the patients showed improvement in CNS-related symptoms in response to conventional immunosuppressive treatment such as intravenous cyclophosphamide pulse treatment (IV-CY), cyclosporine A (CsA), PE and immunoadsorption therapy. All patients completed the course of anti-CD20 antibody treatment described in this study. Patients 1–8, and patients 9 and 10 were treated at the University of Occupational and Environmental Health Hospital and Kyoto University Hospital, respectively, from 2000 to 2005. Informed consent was obtained from all patients in accordance with the regulations of the aforementioned two hospitals, and rituximab was administered in accordance with the study protocol approved by the ethics committee of each hospital.

Abbreviations: CNS, central nervous system; FACS, fluorescence-activated cell sorter; NPSLE, neuropsychiatric systemic lupus erythaematosus; PBS, phosphate-buffered saline; PE, plasma exchange; SLE, systemic lupus erythaematosus; SLEDAI, SLE Disease Activity Index; SPECT, single-photon-emission computed tomography

Treatment protocol

Patients 1–5 and 10 were treated with 375 mg/m^2 rituximab once a week for 2 weeks, and patient 9 received a single administration of the same dose. Patients 6 and 7 received 500 mg rituximab once a week for 4 weeks, while patient 8 was treated with 1000 mg once a week for 2 weeks. Blood pressure and ECG were monitored within the first 3.5 h of the administration to check for any reaction to the drug infusion.

Assessment

Clinical symptoms and treatment-induced adverse reactions were assessed before treatment, every week during treatment, every week within 1 month after treatment and once monthly thereafter. Laboratory tests included blood count, erythrocyte sedimentation rate, liver and renal function tests, urinary protein, serum complement titre and autoantibody level (such as anti-ds-DNA antibody). To evaluate the impact of rituximab on CNS lesions, we measured the immunoglobulin (Ig)G index and interleukin (IL)6 level in the cerebrospinal fluid, MRI, cerebral flood flow scintillator (single-photon-emission computed tomography (SPECT), and ^{18}FTG-positron emission tomography. To assess SLE activity, the SLE Disease Activity Index (SLEDAI) was determined before and after treatment. The level of expression of functional molecules on the lymphocyte cell surface was assessed by flow cytometry.

Flow cytometry

Mononuclear cells were isolated from peripheral blood using lymphocyte separation medium (ICN/Cappel Pharmaceuticals, Aurora, Ohio, USA). After washing twice with phosphate-buffered saline (PBS), the cells were incubated in blocking buffer (0.25% human globulin, 0.5% human albumin (Yoshitomi, Osaka, Japan), and 0.1% NaN_3 (Sigma Aldrich, St Louis, Missouri, USA) in PBS) and left to stand in a 96-well plate at 4℃ for 15 min. In the next step, the cells were incubated in 100 µl of fluorescence-activated cell sorter (FACS) solution (0.5% human albumin and 0.1% NaN_3 in PBS) and then treated with fluorescein isothiocyanate-labelled mouse IgG_1 and antihuman CD40, CD69, inducible costimulator (ICOS), CD19, CD4 (Pharmingen, San Diego, California, USA), CD80 (Chemicon Europe, Chandlers Ford, UK), or CD40L (Ancell, Bayport, USA) antibody, and left to react for 30 min at 4℃. The cells were washed three times with FACS solution and analysed using FACScalibar (Becton–Dickinson, San Jose, California, USA).

Statistical analysis

All data were expressed as mean (SD). Differences between data collected before and after treatment were examined for statistical significance using the Student's t test. $p<0.05$ denoted the presence of a significant difference.

RESULTS

Characteristics of patients

Table 1 summarises the NPSLE classification and laboratory data of the 10 patients. All patients were females with a mean (range) age of 31 (20–55) years. The mean (range) duration of illness from the onset of SLE to administration of rituximab was 9.6 years (3 months to 25 years). Immunosuppressants used for treatment before enrollment in the rituximab protocol included CsA, cyclophosphamide, mizoribine, and azathioprine. In addition, five patients with intractable disease did not respond to the combination treatment, and thus received PE as well.

With regard to CNS-related symptoms, acute confusional state was noted in 5, psychosis in 4, seizures in 2, mood disorders in 2, and one patient each had headache, demyelinating syndrome, myelopathy, anxiety disorder and cognitive dysfunction, based on the NPSLE classification of the American College of Rheumatology.[18 19] MRI findings included abnormal signals in the cerebral white matter in six patients. SPECT showed reduced cerebral blood flow in eight patients. Although a high IgG index[20] was noted in five patients (>0.66), an increase in IL6 was confirmed in only one patient.

Serious haemolytic anaemia, cardiomyopathy-associated decreased cardiac function, muscle pain, mucocutaneous disorders, peripheral neural deficits such as abnormal sensation and neurogenic bladder were also seen in these patients, in addition to the CNS-related changes (tables 1 and 2). In all participants, conventional immunosuppressive therapy produced either no improvement of symptoms or only a poor response. The SLEDAI values (range, 2–49) reflected the presence or absence of organ system-specific activity, with large scores representing involvement of CNS and low scores reflecting haematological activity. In the present study, involvement of organs was limited to those that could be confirmed objectively, while subjective signs such as headache, fatigue and paresthesia were not recorded. Thus, using this approach, the SLEDAI scores of patients with objective signs reflecting multiple involvement of CNS were high whereas those of patients with subjective symptoms only were low. In our study, patients 1 and 3 had multiple CNS signs, patients 1 (49 points) and 3 (37 points) had seizures, psychosis and organic brain syndrome. On the other hand, patient 2 had MRI abnormality in the medulla oblongata but had only paresthesia as a subjective symptom (2 points), and patient 7 had MRI abnormality in the dorsal medulla spinalis and paralysis of the lower extremities, mood and anxiety disorders. However, the SLEDAI scores of both patients were based on subjective symptoms, and thus the scores were low (2 and 3, respectively).

Clinical outcome

At the start of rituximab treatment, patients were treated with low to moderate doses of corticosteroids (15–40 mg of prednisolone, 1–3 mg betamethasone), and continued to use this treatment during the rituximab arm of the study. However, immunosuppressants were stopped at entry to the study in all patients except for patient 8 who continued her treatment of 50 mg azathioprine. The postrituximab follow-up period was 7–45 months. Table 2 provides details of the clinical symptoms and laboratory tests before and 28 days after rituximab treatment (unless otherwise indicated in the table). Improvement in the skin and mucocutaneous lesions was fa... and the ejection fraction recovered from 44% to 72.1% in patient 4. All patients showed improvement in haematopeni... and complement titre and marked falls in PE-resistant autoantibodies after treatment. Analysis of SLE activity before and after the treatment showed a significant decrease in SLEDAI from 19.9 (range, 49–2) before treatment to 6.2 (range, 15–0) after treatment ($p = 0.013$, fig 1). Moreover, SLEDAI decreased to 0 in 9 of the 10 patients at 1–6 months after rituximab treatment.

Rituximab treatment was also effective against CNS lesions in all patients. In particular, the consciousness state of all the five patients who were in acute confusional state before treatment, improved rapidly after the treatment. For example, the GCS score of patient 1 improved from 7–11 to 15 after 5 days of treatment, and that of patient 2 from 3 to 14 after 2 days of treatment. This rapid recovery was clinically significant. In addition, even in three patients who were in a dazed state and needed to be woken up before rituximab treatment, became alert the next day (patient 2) or after a few days of treatment (patients 9 and 10). Furthermore, rituximab also improved neuropsychiatric symptoms such as psychosis

Table 1 Characteristics of 10 female patients with neuropsychiatric systemic lupus erythaematosus at study entry

Patient	Age (years)	Duration of disease	Previous treatment	NP classification	MRI/SPECT	IgG index /IL6 (pg/ml)	Clinical manifestations	SLEDAI
1	35	19 years	CS (40 mg, pulse 14), IV-CY (22), VCR (10 mg), CsA (300 mg, 3 years), AZ (100 mg, 2 months), MTX (8 mg/w, 4 months), PE (11), IA (15)	Acute confusional state, seizure, psychosis	Normal/abnormal	Not done/not done	Fever, fatigue, nephritic syndrome, leukopenia, low Hb, high ESR, CH50, anti-ds DNA ↑	49
2	55	25 years	CS (40 mg, pulse 3), IV-CY (7), PE (2)	Acute confusional state	II, III/abnormal	0.73 ↑ / 1.8	Paresthesia of fingers, severe AIHA, anti-ds DNA ↑	2
3	46	3 months	CS (50 mg), IV-CY (1), PE (2), IA (3)	Acute confusional state, seizure	II, III/abnormal	0.46/33.8 ↑	Leukopenia, low Hb, thrombocytopenia, proteinuria, AIH, anti-ds DNA ↑	37
4	20	1 year	CS (50 mg), CsA (175 mg, 1 m)	Headache	Normal/not done	1.05 ↑ /3.1	Fever, fatigue, skin rash, alopecia, cardiomyopathy, polyneuropathy, leukopenia, C4 ↓, anti-ds DNA ↑	16
5	34	3 years	CS (60 mg), IV-CY (8), MZ (150 mg, 25 months)	Demyelinating syndrome	II, III/normal	0.85 ↑ /0.9	Sensory deficit, photosensitivity, mouth ulcer, lymphocytopenia, C4 ↓	16
6	30	22 years	CS (40 mg), MZ (150 mg, 22 years)	Mood disorder	Normal/abnormal	0.54/1.5	Polyneuropathy, muscular pain, skin rash, leukopenia, anti-ds DNA ↑	17
7	21	7 years	CS (60 mg, pulse 3), IV-CY (14), MTX (intrathecal 30 mg), MZ (300 mg, 2 years)	Myelopathy, mood disorder, anxiety disorder	II, III/abnormal	0.80 ↑ /4.7	Periungual erythaema, leukopenia	3
8	20	9 months	CS (45 mg), IV-CY (6), AZ (50 mg, 1 month)	Psychosis, cognitive dysfunction	III/abnormal	0.56/1.0	Lymphadenopathy, alopecia, malar rash, lymphocytopenia	18
9	20	8 months	CS, CY, DFPP	Acute confusional state, psychosis	III/abnormal	0.98 ↑ /4.2	Fever, lymphadenopathy, low Hb, lymphocytopenia, high ESR, anti-Sm ↑	28
10	29	17 years	CS, AZ, CsA, CY, PE	Acute confusional state, psychosis	Normal/abnormal	0.60/2.4	Severe AIHA, CH50 ↓	18

The disease activity was high in all patients and none had responded to conventional immunosuppressants.

AIHA, autoimmune haemolytic anaemia; AZ, azathioprine; CS, corticosteroid; CsA, cyclosporine; CY, cyclophosphamide; DFPP, double filtration plasmapheresis; ESR, erythrocyte sedimentation rate; Hb, haemoglobin; IA, immunoadsorption; MTX, methotrexate; MZ, mizoribine; PE, plasma exchange; SLE-DAI, Systemic Lupus Erythaematosus Disease Activity Index; VCR, vincristine.

For IV-CY, PE and IA, numbers in parentheses represent the number of treatments. For CS, CsA, AZ and MZ, the doses in parentheses represent maximum dosage. For VCR in patient 1 and MTX in patient 7, the dose in parentheses expresses total dosage.

Table 2 Clinical outcomes of neuropsychiatric systemic lupus erythaematosus after anti-CD20 antibody treatment

Patient	Dose of rituximab	Other treatments at study entry (mg)	CNS manifestations		Objective NPSLE findings after treatment	Duration of remission (m)
			before	after		
1	375 mg/m^2 day 1, 8	Bet 1.0	Consciousness disorder, seizure, psychosis	Complete recovery (GCS 7–11→15/5 days)	Improvement of SPECT	22
2	375 mg/m^2 day 1, 15	Bet 1.5	Consciousness disorder	Improved consciousness	No follow-up data	18
3	375 mg/m^2 day 1, 8	Bet 1.0	Consciousness disorder, seizure	Complete recovery (GCS 3→14/2 days)	No improvement in MRI and SPECT	23
4	375 mg/m^2 day 1, 8	m-PSL 20	Headache	Resolution of headache	Improved IgG index (1.05 →0.84/4 w)	29
5	375 mg/m^2 day 1, 8	Bet 1.25	Paresthesia of fingers, toes and left precordial-back	Resolution of paresthesia	Improvement of neck MRI	7
6	500 mg day 1, 8, 15, 22	Bet 2.5	Depressive state, insomnia	Improvement of depressive state	Improvement of SPECT	7
7	500 mg day 1, 8, 15, 22	Bet 1.25	Paresis of both lower limbs, muscle weakness, depressive state	Reduction of paresis, improvement of depressive state (SDS 58→50/2 w)	Improvement of SPECT, improvement of IgG index (0.80 →0.72/3 m)	14
8	1000 mg day 1, 15	Bet 1.25, AZ 50	Psychosis, cognitive dysfunction	Improvement of psychosis (BPRS 26→7/8 w)	Improvement of SPECT	11
9	375 mg/m^2 day 1	PSL 45	Consciousness disorder, psychosis, paresis of both lower limbs, neurological bladder	Complete recovery	Improvement of PET and MRI, improved IgG index (0.98 →0.61/2 w)	10
10	375 mg/m^2 day 1, 8	Bet 3	Consciousness disorder, hallucination, cataplexy	Complete recovery	No significant improvement in objective findings	4

Bet, betamethasone; BPRS, brief psychiatric rating scale; CNS, central nervous system; GCS, Glasgow Coma Scale; m-PSL, methylprednisolone; MRI, magnetic resonance imaging; NPSLE, neuropsychiatric systemic lupus erythaematosus; PET, 18FTG-positron emission tomography; PSL, prednisolone; SDS, self-rating depression scale; SPECT, single photon emission computed tomography. For other abbreviations, see table 1.

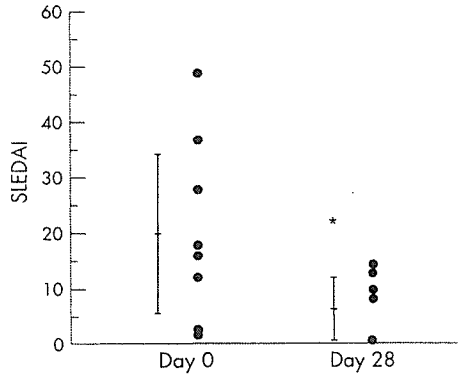

Figure 1 Systemic lupus erythaematosus disease activity index (SLEDAI) score before and 28 days after rituximab treatment. A decrease in SLEDAI score was detected in 9 of the 10 patients. Data are mean (SD). *p<0.05.

and mood disorder within a few weeks to a few months after treatment. For example, the Brief Psychiatric Rating Scale, which is used for the assessment of schizophrenia, markedly decreased in patient 8 from 26 to 7 points within 2 months, together with recovery of communication skills. In addition, patients 1 and 9 showed rehabilitation into society after rituximab treatment although they had serious neuropsychiatric symptoms before treatment. In addition to the improvement in SLE activity and clinical symptoms, rituximab also improved the quality of life of the patients.

We also assessed the effects of rituximab treatment by comparing the findings of MRI and SPECT before and after treatment. In four patients (patients 1, 6, 7 and 8), rituximab treatment improved cerebral blood flow as determined by SPECT; in patient 1, such improvement was noted at the early stage of treatment and paralleled the improvement in clinical symptoms. For patient 5, rituximab treatment resulted in improvement in the abnormal findings in T2-weighted images of the cervical cord on MRI, along with the improvement in sensory deficits due to inflammation at the same site. For patient 9, rituximab treatment resulted in reduction of the high-intensity lesion in the head MRI T2-weighted image.

Five of our patients had peripheral neuropathies in addition to CNS lesions. Treatment with rituximab resulted in remission or marked improvement of paresthesia in patient 2, radiculopathy in patient 4, ulnar neuropathy in patient 6, and neurological bladder in patient 9. Rituximab also improved quality of life based on improvement of peripheral neuropathy-related symptoms although such symptoms tended to persist after treatment.

While the overall therapeutic effect of rituximab was excellent, some patients developed relapse after long-term remission. Six of the 10 patients showed reactivation of SLE including reappearance of CNS-related symptoms. For patient 1, remission was maintained with low-dose steroid for 22 months after rituximab treatment. However, the patient showed recurrence associated with an increase in autoantibodies and proteinuria. Recurrence was also noted 18 months after treatment in patient 2, associated with haemolysis. Both patients 1 and 2 required retreatment with rituximab. At 23 months after completion of rituximab treatment, patient 3 showed worsening of the head MRI findings and cerebrospinal fluid abnormalities and developed witnessed seizure attacks. In patient 5, a reduction in the steroid dose was followed by recurrence of CNS-related symptoms after 7 months. Generalised skin rashes appeared in patient 9 after 10 months and patient 10 reported worsening of lupus headache after 4 months. Patients 3 and 5 received IV-CY treatment, and patient 9 and 10 required an increase in the steroid dose. However, four patients (patients 4, 6, 7 and 8) maintain a remission state at the time of writing this report (at 35 months in patient 4, at 7 months in patient 6, at 19 months in patient 7 and 16 months in patient 8) after the completion of rituximab treatment.

Adverse effects

Of the 10 patients, two developed pneumonia, one had herpes zoster, one developed chickenpox and one had intractable infection of decubitus ulceration. These infections were successfully controlled with antibiotics.

Phenotypic analysis of SLE lymphocytes

T cells and B cells are activated by antigen stimulation via T cell receptors and signals from costimulatory molecules. The responsible costimulatory molecules, such as CD40/40L, CD80, CD86/CD28 and ICOS/B7h, are known to be expressed in patients with active SLE.[21–26]

We performed serial analysis of the expression of functional molecules in eight patients with SLE before and after rituximab treatment by flow cytometry. Rituximab treatment resulted in rapid disappearance of CD20, a specific antigen to B cells, marked decrease in CD19-positive cells, within several days to 2 weeks after treatment. Rituximab also resulted in rapid falls in the percentages of CD40-expressing and CD80-expressing CD19 cells within 1 day and both were hardly detected after the second day (fig 2). The expression levels of these molecules were still low at 3 months after completion of rituximab treatment.

We also assessed the effects of treatment on the expression levels of CD40L (a costimulatory molecule on CD4-positive cells), ICOS and CD69 (an early activation antigen). While only three patients showed high expression of these molecules before treatment, rituximab treatment reduced the expression levels of these molecules in all three patients (fig 3), suggesting that rituximab does not only affect B cells but also T cells in patients with SLE.

DISCUSSION

To date, reports on rituximab treatment for autoimmune diseases have covered various conditions, including RA, SLE, dermatomyositis, Sjögren's syndrome and vasculitis.[27–30] Rituximab treatment resulted in improvement, manifested by a decrease in the British Disease Activity score and SLE DAI score, of arthropathy, nephropathy, thrombocytopenia and haemolytic anaemia.[11–16]

Although few reports described the efficacy of rituximab treatment in patients with SLE with CNS lesions,[11 14 31] to our knowledge, there are no published reports that provide detailed analysis of the effects of such treatment in a large group of patients. Rituximab has a large molecular weight of 146 kDa, and hence cannot readily cross the blood–brain barrier; therefore, it is unlikely to reach the cerebrospinal fluid following systemic administration. We measured rituximab concentration in the cerebrospinal fluid of patient 8 at 24 h after treatment. The value (0.3 μg/ml) was slightly higher than the lower detection limit of the assay, whereas the serum concentration was 279 μg/ml. Based on this finding, we assume that the central effects of rituximab are mediated through another mechanism, not through antibody-dependent cellular cytotoxicity and/or complement-dependent cytotoxicity.[32]

To assess autoreactive lymphocyte activity, we determined the expression of various functional molecules on the surface of peripheral blood lymphocytes before and after rituximab treatment by using flow cytometry. We previously proposed that rituximab could regulate SLE disease activity and correct

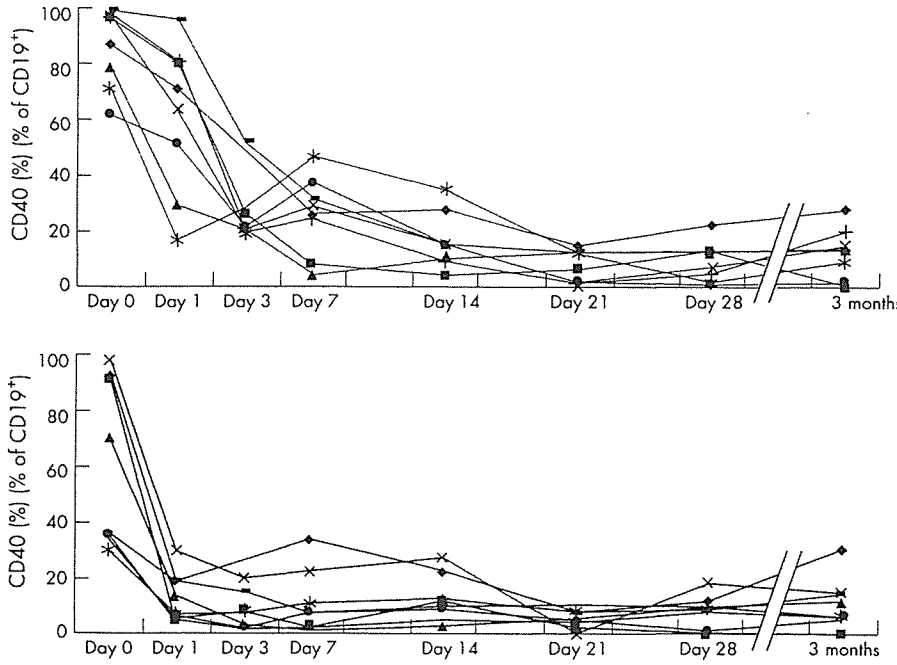

Figure 2 Serial changes in CD40 and CD80 expression on CD19-positive cells after rituximab treatment in eight patients with systemic lupus erythaematosus. CD40 and CD80 expression was measured before and 28 days after rituximab treatment.

autoimmune abnormalities.[12] The present results showed a rapid decrease in the expression of functional surface molecules and maintenance of long-term control following rituximab treatment (fig 2). Specifically, a marked decrease in the proportion of CD40-expressing and CD80-expressing cells was detected on the day after initiation of rituximab treatment. In this regard, Leng *et al*[33] found CD40 overexpression in CD19 cells in patients with rheumatoid arthritis compared with healthy controls. Others also reported that the percentage of CD80-positive cells among activated B cell subset was higher in SLE than the controls.[34] These results suggest that the target of rituximab treatment is activated B cells. Anolik *et al*[35] examined B cell phenotypes after rituximab treatment and reported that the proportion of autoreactive memory B cells was decreased after rituximab treatment. Considered together, the above results and those of the present study suggest that T cell activation is negatively influenced by a rapid decrease in B cell to T cell stimulation in parallel with the loss of B cells. Our

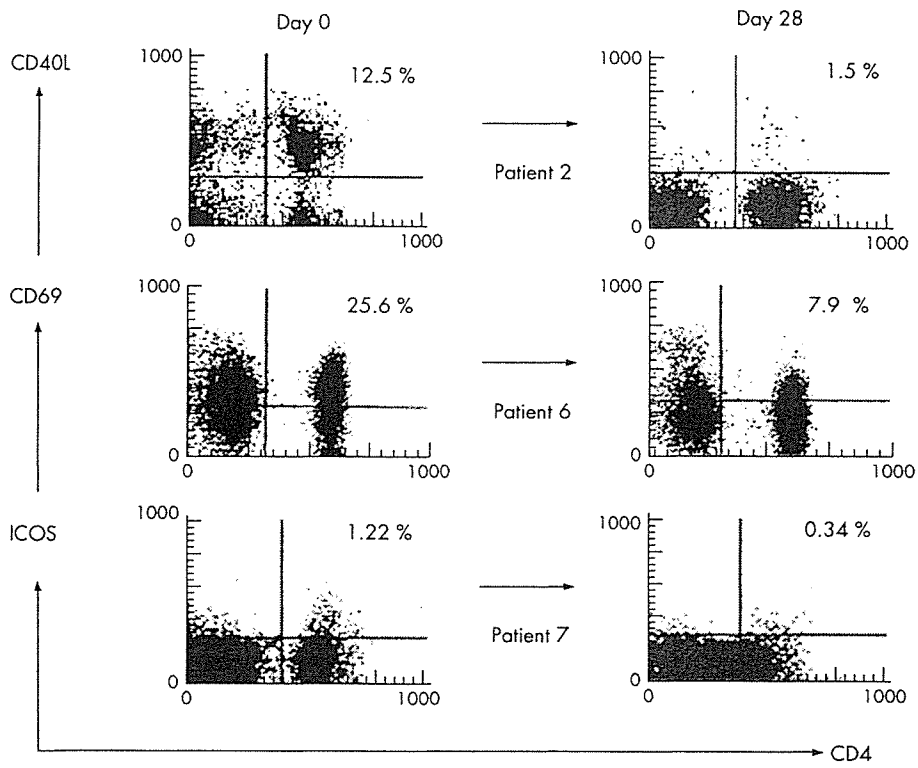

Figure 3 Changes in expression of functional molecules on CD4-positive cells induced by rituximab treatment. The expression of CD40L (patient 2), CD69 (patient 6) and ICOS (patient 7) on CD4-positive cells was measured before (day 0) and 28 days after rituximab treatment. Percentages represent the percentage of CD4-positive cells expressing the functional molecules.

results also showed that rituximab down regulated CD40L, ICOS and CD69 on CD4-positive cells in patients with active SLE (fig 3). Sfikakis *et al*[36] also reported that rituximab treatment decreased CD40L and CD69 expression in patients with SLE. These results imply that rituximab could eliminate B cells bearing functional molecules and inhibit the interaction between these B cells and activated T cells by down regulating costimulatory molecules, and also possibly by reducing the production of certain cytokines and complement activation, which could lead to rapid improvement of CNS manifestations of the disease.

At present, there is no treatment strategy for patients with NPSLE who fail to respond to conventional therapies. In such patients, large doses of steroids are provided on long-term basis, and IV-CY is administered continuously. Our study showed that rituximab is useful as a new treatment for such cases. However, recurrence after rituximab treatment was noted in our patients, as has been reported previously in patients with rheumatoid diseases.[28] Two of our patients who experienced recurrence received rituximab re-treatment. However, these patients experienced recurrence at 18 and 22 months after rituximab treatment, suggesting that remission could be maintained for a comparatively long period of time with rituximab treatment. Further studies are needed to develop strategies for the prevention of recurrence and counter measures for inhibiting the production of antichimeric antibodies.[37 38] There is also a need to investigate the long-term effects of rituximab treatment and its organ specificity.

ACKNOWLEDGEMENTS

This work was supported in part by a Research Grant-In-Aid for Scientific Research by the Ministry of Health, Labor and Welfare of Japan, the Ministry of Education, Culture, Sports, Science and Technology of Japan and University of Occupational and Environmental Health, Japan.

Authors' affiliations

Mikiko Tokunaga, Kazuyoshi Saito, Shingo Nakayamada, Shizuyo Tsujimura, Masao Nawata, Shigeru Iwata, Taeko Azuma, Yoshiya Tanaka, The First Department of Internal Medicine, School of Medicine, University of Occupational and Environmental Health, Kitakyusyu, Japan
Daisuke Kawabata, Yoshitaka Imura, Takao Fujii, Tsuneyo Mimori, Department of Rheumatology and Clinical Immunology, Kyoto University, Graduate School of Medicine, Kyoto, Japan

Competing interests: None declared.

REFERENCES

1 **Blanco FJ**, Gomez-Reino JJ, de la Mata J, *et al*. Survival analysis of 306 European Spanish patients with systemic lupus erythematosus. *Lupus* 1998;**7**:159–63.
2 **Kasitanon N**, Louthrenoo W, Sukitawut W, *et al*. Causes of death and prognostic factors in Thai patients with systemic lupus erythematosus. *Asian Pac J Allergy Immunol* 2002;**20**:85–91.
3 **Hahn BH**. Systemic lupus erythematosus. In: Kasper DL, eds. *Origins of Harrison's principles of internal medicine*.16th edn. Columbus: McGraw-Hill, 2005:1960–7.
4 **Ad Hoc Working Group on Steroid-Sparing Criteria in Lupus**. Criteria for steroid-sparing ability of interventions in systemic lupus erythematosus: report of a consensus meeting. *Arthritis Rheum* 2004;**50**:3427–31.
5 **Goldblatt F**, Isenberg DA. New therapies for systemic lupus erythematosus. *Clin Exp Immunol* 2005;**140**:205–12.
6 **Petri M**. Cyclophosphamide: new approaches for systemic lupus erythematosus. *Lupus* 2004;**13**:366–71.
7 **Boumpas DT**, Yamada H, Patronas NJ, *et al*. Pulse cyclophosphamide for severe neuropsychiatric lupus. *Q J Med* 1991;**81**:975–84.
8 **Barile-Fabris L**, Ariza-Andraca R, Olguin-Ortega L, *et al*. Controlled clinical trial of IV cyclophosphamide versus IV methylprednisolone in severe neurological manifestations in systemic lupus erythematosus. *Ann Rheum Dis* 2005;**64**:620–5.
9 **Sherer Y**, Levy Y, Longevitz P, *et al*. Successful treatment of systemic lupus erythematosus cerebritis with intravenous immunoglobulin. *Clin Rheumatol* 1999;**18**:170–3.
10 **Valesini G**, Priori R, Francia A, *et al*. Central nervous system involvement in systemic lupus erythematosus: a new therapeutic approach with intrathecal dexamethasone and methotrexate. *Springer Semin Immunopathol* 1994;**16**:313–21.
11 **Saito K**, Nawata M, Nakayamada S, *et al*. Successful treatment with anti-CD20 monoclonal antibody (rituximab) of life-threatening refractory systemic lupus erythematosus with renal and central nervous system involvement. *Lupus* 2003;**12**:798–800.
12 **Tokunaga M**, Fujii K, Saito K, *et al*. Down-regulation of CD40 and CD80 on B cells in patients with life-threatening systemic lupus erythematosus after successful treatment with rituximab. *Rheumatology* 2005;**44**:176–82.
13 **Perrotta S**, Locatelli F, La Manna A, *et al*. Anti-CD20 monoclonal antibody (Rituximab) for life-threatening autoimmune haemolytic anaemia in a patient with systemic lupus erythematosus. *Br J Haematol* 2002;**116**:465–7.
14 **Leandro MJ**, Edwards JC, Cambridge G, *et al*. An open study of B lymphocyte depletion in systemic lupus erythematosus. *Arthritis Rheum* 2002;**46**:2673–7.
15 **Looney RJ**, Anolik JH, Campbell D, *et al*. B cell depletion as a novel treatment for systemic lupus erythematosus: a phase I/II dose-escalation trial of rituximab. *Arthritis Rheum* 2004;**50**:2580–9.
16 **Leandro MJ**, Cambridge G, Edwards JC, *et al*. B-cell depletion in the treatment of patients with systemic lupus erythematosus: a longitudinal analysis of 24 patients. *Rheumatology* 2005;**44**:1542–5.
17 **Tan EM**, Cohen AS, Fries JF, *et al*. The 1982 revised criteria for the classification of systemic lupus erythematosus. *Arthritis Rheum* 1982;**25**:1271–7.
18 **ACR Ad Hoc Committee on Neuropsychiatric Lupus Nomenclature**. The American College of Rheumatology nomenclature and classification and case definitions for neuropsychiatric lupus syndromes. *Arthritis Rheum* 1999;**42**:599–608.
19 **Borchers AT**, Aoki CA, Naguwa SM, *et al*. Neuropsychiatric features of systemic lupus erythematosus. *Autoimmun Rev* 2005;**4**:329–44.
20 **French CA**, Tracy RP, Rudick RA, *et al*. Simultaneous determination of cerebrospinal fluid oligoclonal bands and the "gamma-protein index" by agarose electrophoresis and densitometry. *Clin Chem* 1986;**32**:84–7.
21 **Datta SK**, Kalled SL. CD40-CD40 ligand interaction in autoimmune disease. *Arthritis Rheum* 1997;**40**:1735–45.
22 **Koshy M**, Berger D, Crow MK. Increased expression of CD40 ligand on systemic lupus erythematosus lymphocytes. *J Clin Invest* 1996;**98**:826–37.
23 **Yellin MJ**, Thienel U. T cells in the pathogenesis of systemic lupus erythematosus: potential roles of CD154-CD40 interactions and costimulatory molecules. *Curr Rheumatol Rep* 2000;**2**:24–31.
24 **Kovacs B**, Thomas DE, Tsokos GC. Elevated *in vivo* expression of the costimulatory molecule B7-BB1 (CD80) on antigen presenting cells from a patient with SLE. *Clin Exp Rheumatol* 1996;**14**:695–7.
25 **Bijl M**, Horst G, Limburg PC, *et al*. Expression of costimulatory molecules on peripheral blood lymphocytes of patients with systemic lupus erythematosus. *Ann Rheum Dis* 2001;**60**:523–6.
26 **Andreas H**, Kerstin B, Karin R, *et al*. Involvement of inducible costimulator in the exaggerated memory B cell and plasma cell generation in systemic lupus erythematosus. *Arthritis Rheum* 2004;**50**:3211–20.
27 **Leandro MJ**, Edwards JC W, Cambridge G. Clinical outcome in 22 patients with rheumatoid arthritis treated with B lymphocyte depletion. *Ann Rheum Dis* 2002;**61**:883–8.
28 **Keogh KA**, Ytterberg SR, Fervenza FC, *et al*. Rituximab for refractory Wegener's granulomatosis: report of a prospective, open-label pilot trial. *Am J Respir Crit Care Med* 2006;**173**:180–7.
29 **Levine TD**. Rituximab in the treatment of dermatomyositis: an open-label pilot study. *Arthritis Rheum* 2005;**52**:601–7.
30 **Pijpe J**, van Imhoff GW, Spijkervet FK, *et al*. Rituximab treatment in patients with primary Sjogren's syndrome: an open-label phase II study. *Arthritis Rheum* 2005;**52**:2740–50.
31 **Armstrong DJ**, McCarron MT, Wright GD. SLE-associated transverse myelitis successfully treated with Rituximab (anti-CD20 monoclonal antibody). *Rheumatol Int* 2005;**18**:1–2.
32 **Reff ME**, Carner K, Chambers KS, *et al*. Depletion of B cells in vivo by a chimeric mouse human monoclonal antibody to CD20. *Blood* 1994;**83**:435–45.
33 **Leng JH**, Hu ZY, Zhuo GC, *et al*. The expression and significance of costimulatory molecule in peripheral blood B lymphocytes in rheumatoid arthritis. *Zhonghua Nei Ke Za Zhi* 2004;**43**:519–21.
34 **Folzenlogen D**, Hofer MF, Leung DY, *et al*. Analysis of CD80 and CD86 expression on peripheral blood B lymphocytes reveals increased expression of CD86 in lupus patients. *Clin Immunol Immunopathol* 1997;**83**:199–204.
35 **Anolik JH**, Barnard J, Cappione A, Pugh-Bernard AE, *et al*. Rituximab improves peripheral B cell abnormalities in human systemic lupus erythematosus. *Arthritis Rheum* 2004;**50**:3580–90.
36 **Sfikakis PP**, Boletis JN, Lionaki S, *et al*. Remission of proliferative lupus nephritis following B cell depletion therapy is preceded by down-regulation of the T cell costimulatory molecule CD40 ligand: an open-label trial. *Arthritis Rheum* 2005;**52**:501–13.
37 **Weide R**, Heymanns J, Pandorf A, *et al*. Successful long-term treatment of systemic lupus erythematosus with rituximab maintenance therapy. *Lupus* 2003;**12**:779–82.
38 **Edelbauer M**, Jungraithmayr T, Zimmerhackl LB. Rituximab in childhood systemic lupus erythematosus refractory to conventional immunosuppression: case report. *Pediatr Nephrol* 2005;**20**:811–13, .

Mod Rheumatol (2006) 16:44–47
DOI 10.1007/s10165-005-0447-1

CASE REPORT

Hide Yoshida · Hirahito Endo · Sumiaki Tanaka
Akira Ishikawa · Hirobumi Kondo · Takeshi Nakamura

Recurrent paralytic ileus associated with strongyloidiasis in a patient with systemic lupus erythematosus

Received: October 7, 2005 / Accepted: November 22, 2005

Abstract We present an interesting case of recurrent paralytic ileus due to strongyloidiasis in a woman who was being treated with corticosteroids and immunosuppressants for systemic lupus erythematosus (SLE). She was also a carrier of human T-cell leukemia virus type I. She had a history of strongyloidiasis 8 years earlier. Recurrent episodes of paralytic ileus due to strongyloidiasis occurred during treatment of her SLE with corticosteroids. Ivermectin was given and improved the symptoms. This case shows that symptomatic strongyloidiasis can be induced in immunocompromised hosts by immunosuppressive therapy. It is important to rule out strongyloidiasis prior to starting immunosuppressive therapy in patients from endemic areas.

Key words Corticosteroids · Cyclophosphamide · Human T-cell leukemia virus type I (HTLV-I) · Paralytic ileus · Strongyloidiasis · Systemic lupus erythematosus (SLE)

Introduction

Strongyloidiasis is a disease of tropical regions, so the endemic areas in Japan are Okinawa and Amami. *Strongyloides stercoralis* infection is observed in 11.2% of the inhabitants of these regions.[1] Many of the symptomatic patients are considered to be immunocompromised hosts. Patients with strongyloides can develop ileus, protein-losing enteropathy, and diarrhea, especially when treated with immunosuppressants or corticosteroids, while severe strongyloidiasis is occasionally fatal as a result of systemic infection. We report an interesting case of strongyloidiasis in a woman from Okinawa. She had a history of strongyloidiasis 8 years earlier. When she was treated with corticosteroids for systemic lupus erythematosus (SLE), recurrent paralytic ileus occurred and was later revealed to be due to strongyloidiasis. Ivermectin was given and improvement of her symptoms was noted. Immunosuppressive therapy with steroids or chemotherapeutic agents may cause symptomatic strongyloidiasis in susceptible patients.

H. Yoshida (✉) · H. Endo · S. Tanaka · A. Ishikawa · H. Kondo
Division of Rheumatology, Department of Internal Medicine, Kitasato University School of Medicine, 1-15-1 Kitasato, Sagamihara, 228-8555, Japan
Tel. +81-42-778-8111; Fax +81-42-778-9465
e-mail: yhide@med.kitasato-u.ac.jp

T. Nakamura
Department of Microbiology and Parasitology, Kitasato University School of Medicine, Sagamihara, Japan

Case report

A 54-year-old Japanese woman was admitted to Kitasato University Hospital for evaluation and treatment of lupus nephritis on February 2004. She had been born in Okinawa Prefecture. In 1976, she emigrated to Brazil and worked as a farmer. In 1986, she returned to Japan and lived in Kanagawa Prefecture as a housewife. From 1990, she noted episodes of abdominal fullness, but these improved without treatment. In April 1994 she visited a local hospital, suffering abdominal distension and pain for ileus.

Because she continued to have episodes of abdominal distension, she attended the Department of Gastroenterology at Kitasato University East Hospital in September 1994. Gastroduodenoscopy showed enteritis, and *Strongyloides* larvae were identified in mucosal specimens obtained by biopsy, so she was diagnosed as having paralytic ileus due to strongyloidiasis. In December 1994, she was treated with mebendazole (100 mg twice a day). Treatment was continued intermittently over about 8 months. After the completion of treatment, stool examination did not detect strongyloides.

In 2000 she visited a local hospital, with a respiratory tract infection. Blood tests were performed and thrombocytopenia was noted. She was referred to the Department of Rheumatology at Kitasato University Hospital. Systemic lupus erythematosus was diagnosed by polyarthritis and laboratory tests (positive for antinuclear antibodies and anti-DNA antibodies, as well as having pancytopenia). In 2001, her polyarthritis and pancytopenia worsened, so she

started treatment with prednisolone (PSL) at 15 mg/day. In February 2004 (the PSL dose was 8 mg/day), urinalysis revealed red blood cell casts and proteinuria. In September, she was admitted to our hospital for evaluation and treatment. Physical examination showed a middle-aged woman with a temperature of 36.0°C, heart rate of 62 beats/min, respiration rate of 14 breaths/min, and blood pressure of 158/92 mmHg. No pulmonary or abdominal abnormalities were found. She had noted a weight gain of 2 kg (her weight was 51.9 kg) and pretibial edema. The electrocardiogram and chest X-ray film were normal. On admission, laboratory tests showed a hemoglobin of 9.0 g/dl and a white blood cell count of 4600/μl (81.9% neutrophils, 12.1% lymphocytes, 2.0% eosinophils, and 4.0% monocytes). Urinalysis showed 3+ proteinuria and 2+ hematuria. Examination of the sediment showed 8–10 erythrocytes per high-power field, 5–10 leukocytes per high-power field, granular casts, and hyaline casts. She also had proteinuria (5.5 g/day), a total protein of 5.5 g/dl, serum albumin of 2.5 g/dl, serum creatinine of 0.8 mg/dl, and daily creatinine clearance of 54.7 ml/min. Stools were negative for occult blood and microscopy of a stool sample was not performed. The complement levels were normal: C3 was 71 mg/dl (normal: 76–160), C4 was 9 mg/dl (normal: 14–44), and CH_{50} was 19 IU/ml (normal: 25–45). Antinuclear antibody was positive at a titer of 1:1280 (both the homogeneous type and the speckled type). Anti-DNA antibody was also positive at 77 IU/ml, but HBs antigen and anti-HCV antibody were negative. Ultrasonography showed normal-sized kidneys and no ascites or pericardial effusion.

Percutaneous renal biopsy was performed 14 days after hospitalization, and was diagnosed as lupus nephritis (Class IV-S(A/C): active and chronic lesions: diffuse proliferative and sclerosing lupus nephritis in the 2003 classification of lupus nephritis). She was treated with methylprednisolone (mPSL) at 500 mg for 3 days, followed by prednisolone at 50 mg/day. On the 40th hospital day, her proteinuria decreased to 2 g/day and there was 1+ hematuria. Because of sustained proteinuria, she was treated with intravenous cyclophosphamide (500 mg) on the 47th hospital day. On the 68th hospital day, she developed vomiting. On examination, no bowel sounds were heard. Abdominal X-ray films showed an abnormal gas collection in a large and small bowel with niveau under the diagnosis of paralytic ileus (Fig. 1). Conservative treatment was provided (fasting, continuous suction through a nasogastric tube, and intravenous infusion). Her symptoms improved after gastric tube insertion, but stool examination was performed because there was a history of strongyloidiasis. Stools were positive for occult blood, and microscopic examination of a stool sample revealed *Strongyloides* larvae (Fig. 2A,B). On the 71st hospital day, gastroduodenoscopy showed duodenal inflammation, and biopsy revealed *Strongyloides* larvae in the mucosa. Paralytic ileus due to strongyloidiasis was diagnosed, and she was given 6 mg of Ivermectin on the 70th and 84th hospital days. Microscopic examination of a stool sample demonstrated no *Strongyloides* larvae on the 84th hospital day. Then it was noticed that her human T-cell leukemia virus type I (HTLV-I) antibody titer was >356.

Fig. 1. X-ray film of the abdomen showed niveau of the small intestine, the so-called herring-bone sign

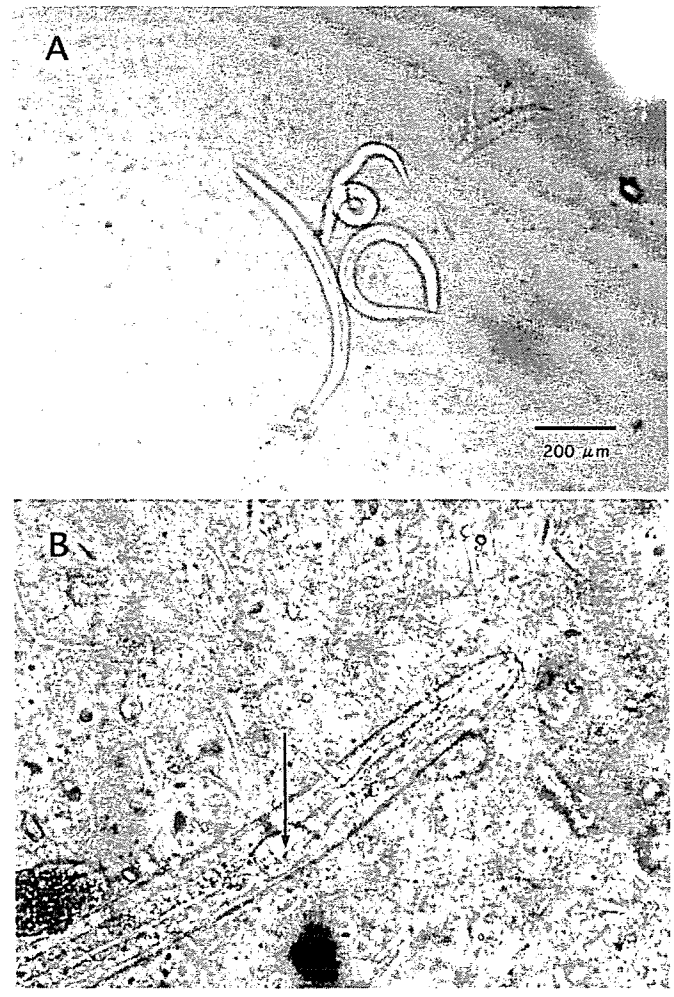

Fig. 2. A Rhabditiform larva of *Strongyloides stercoralis* separated from the stool of the patient. **B** The larva had a muscular esophageal structure, indicated by the *arrow*

Peripheral blood adult T-cell leukemia (ATL) cells were negative throughout the clinical course. We gave a second intravenous cyclophosphamide pulse (500 mg) on the 96th hospital day and microscopic examination of a stool sample subsequently demonstrated no *Strongyloides* larvae. On the 100th hospital day, she was discharged on PSL at 15 mg/day. Urinalysis showed 1+ proteinuria (0.7 g/day) and 1+ hematuria, while the sediment contained 1–5 leukocytes per high-power field. Other tests showed the following: total protein 5.4 g/dl, serum albumin 3.6 g/dl, serum creatinine 0.6 mg/dl, and daily creatinine clearance 74.8 ml/min. The C3, C4, and CH_{50} levels were 61 mg/dl, 14 mg/dl, and 28 IU/ml, respectively, and anti-DNA antibody was positive at 3 IU/ml. Since the patient's discharge from hospital, larvae have not been discovered in the stool.

Discussion

Strongyloidiasis is a parasitic infection caused by *Strongyloides stercoralis*, which is distributed widely in tropical and subtropical areas. South Kyushu and Okinawa are the regions where it commonly occurs in Japan, and it was reported that strongyloidiasis affects 11.2% of the inhabitants.[1] *Strongyloides stercoralis* has two parts to its life cycle: free-living and parasitic. Infectious filariform larvae invade percutaneously and travel via the blood or lymph to the lungs. After passing into the airways, the larvae are swallowed and then inhabit the mucosa of the duodenum and proximal jejunum. In addition, so-called autoinfection occurs when filariform larvae metamorphose in the bowel and reinfect the bowel. The infection thus continues throughout life or for many years with new generations of parasites owing to autoinfection. Disseminated strongyloidiasis can occur when the host becomes seriously ill.[2] To make a diagnosis of strongyloidiasis, the parasite should be detected in the stools or duodenal juice, or the ova should be found. In addition, endoscopic examination may allow diagnosis by detecting parasites in the duodenum, or by biopsy of atypical inflammatory changes of the jejunal mucosa.[3] In our present case, we were able to prove the diagnosis by stool examination and duodenal biopsy. Symptoms of strongyloidiasis are not specific, but diarrhea, loose stools, abdominal pain, malaise, and loss of weight are common.[2] In severe cases, paralytic ileus can develop. Paralytic ileus in our case may have been caused by massive intestinal infestation with *Strongyloides stercoralis*.[4]

There have been 25 reported cases of strongyloidiasis-related ileus (15 in Japan and 10 in foreign countries). The age at diagnosis was 2–82 years, with elderly and middle-aged (>50 years old) patients accounting for about half. There were 15 males and 10 females. Recurrent ileus was not reported overseas, but was found in 3/15 cases in Japan. The risk factors for strongyloidiasis include (1) immunosuppressive therapy (chronic steroid administration), (2) malignancy, (3) immune deficiency (malignant lymphoma, adult T-cell leukemia/lymphoma, etc.),[5] (4) organ transplantation, (5) surgery, (6) pregnancy/delivery, (7) nutritional deficiency and chronic alcoholism, and (8) other causes (diabetes mellitus, SLE, anti HTLV-1 antibody).[6] Among these factors, immunosuppressive therapy was performed for 4/15 cases in Japan and 4/10 overseas. In addition, HTLV-I antibody was positive in 6/15 cases in Japan, but was negative (or not investigated) in the overseas cases. Okinawa is an endemic area for HTLV-I. Nakada et al. reported that 39% of patients with *Strongyloides stercoralis* infestation were positive for HTLV-I proviral DNA, and suggested that *Strongyloides* and HTLV-I-infected cells or HTLV-I itself may interact with each other, or that depression of cell-mediated immunity by HTLV-I allows the development of *Strongyloides* hyperinfestation.[7] Our patient was also seropositive for HTLV-I.

Systemic lupus erythematosus patients are immunocompromised hosts, but they rarely develop strongyloidiasis, and we found only 10 reports during our search of the literature (Table 1).[8–17] The duration of SLE before the onset of strongyloidiasis was variable (5 weeks to 12 years), but all of the patients reported therapeutic contents were using corticosteroids. Symptoms that resembled those of

Table 1. Case reports of *Strongyloides stercoralis* in patients with systemic lupus erythematosus

Sex	Age (years)	Disease duration	Therapy	Nematode search specimen	Outcome	Area	First author[Ref.]
F	18	NR	PSL 60 mg/day + IVCY 1 g/month	Stool, sputum	Survived	Australia	Potter[8]
NR	NR	3 y	NR	NR	Died	USA	Lemos[9]
F	38	2 y	PSL 20 mg/day	Blood vessel	Died	USA	Reiman[10]
F	67	1 y	PSL 15 mg/day	Sputum, stomach, intestines	Died	Japan	Setoyama[11]
F	44	12 y	NR	Sputum, duodenum, lymph node	Died	Argentina	Finkielman[12]
F	43	4 m	PSL	Sputum, stool	Died	USA	Livneh[13]
M	59	7 y	PSL 30 mg/80 mg (alternative day)	Stool, sputum	Survived	USA	Wachter[14]
F	43	2 y	PSL 30 mg/day	NR	Survived	USA	Webster[15]
M	66	5 w	PSL 120 mg/day	Jejunum	Survived	USA	Berger[16]
M	23	3 y	PSL 60 mg/day	Duodenum, stool	Survived	USA	Rivera[17]
F	51	4 y	PSL 35 mg/day	Duodenum, stool	Survived	Japan	Present case

Age, age at onset of disease; NR, not recorded; PSL, prednisolone; IVCY, intravenous cyclophosphamide; y, years; m, months; w, weeks

SLE were found occasionally, such as abdominal pain, respiratory failure, and cerebral disease. Accordingly, when we encounter such symptoms, we have to distinguish a flare-up of SLE disease activity from strongyloidiasis. The present patient was diagnosed as having active SLE and was treated with high-dose corticosteroids and intravenous cyclophosphamide pulse therapy. This treatment plus being an HTLV-1 carrier induced the development of strongyloidiasis.

Strongyloidiasis causes anemia, eosinophilia, hypocholesterolemia (due to abnormal fat absorption), and hypoalbuminemia (due to protein-losing enteropathy).[18] Anemia and hypoalbuminemia were found in our patient, but there is a possibility that these changes developed with increased SLE activity (lupus nephritis, etc.), and distinguishing the symptoms of SLE from strongyloidiasis is difficult. Although our patient had the nephrotic syndrome, her cholesterol level was lower at the time of hospitalization, so we cannot exclude the possibility of latent *Strongyloides stercoralis* infestation. On the other hand, eosinophilia is not found in serious cases[19] or cases treated with corticosteroids,[20] even if there is infestation with *Strongyloides stercoralis*. Because eosinophilia was not found in our case, it seems difficult to judge the presence or absence of *Strongyloides stercoralis* only on the basis of eosinophilia in patients on systemic steroid therapy.

In recent years, the occurrence of nephrotic syndrome due to strongyloidiasis itself has been suggested. Mori et al.[21] reported a nephrotic syndrome patient with eosinophilia who developed ileus, epigastralgia, and malabsorption due to strongyloidiasis. Percutaneous renal biopsy revealed minimal change nephrotic syndrome and the patient recovered with Thiabendazole treatment. In the present case, rather than strongyloidiasis, it seems likely that nephritis was a symptom of SLE, because it developed along with markers of increased disease activity such as an increased anti-DNA antibody titer, hypocomplementemia and renal pathological findings.

As pharmacotherapy for this patient, we used Ivermectin (6mg) orally twice every 2 weeks. No *Strongyloides* larvae were seen on microscopic examination of stool samples after the first treatment on the fourth day. In recent years, oral Ivermectin has been increasingly used for strongyloidiasis,[22] but it is clear that its efficacy is lower in patients with a greater disease burden.[23]

In conclusion, our case emphasizes that immunosuppressed individuals treated with immunosuppressants should be assessed for possible parasite infestation by stool examination prior to starting therapy, if the patient was a resident or born in endemic areas.

References

1. Asato R, Nakasone T, Yoshida C. Current status of *Strongyloides* infection in Okinawa, Japan. Jpn J Trop Med Hyg 1992;20:169–73.
2. Saito A. New diagnostic procedure and cure for strongyloidiasis. Jpn J Infect Dis 1996;70:876–7.
3. Bannon JP, Fater M, Solit R. Intestinal ileus secondary to *Strongyloides stercoralis* infection: case report and review of the literature. Am Surg 1995;61:377–80.
4. De Palola D, Dias LB, Da Silva JR. Enteritis due to *Strongyloides stercoralis* – A report of 5 fatal cases. Am J Dig Dis 1962;7:1086.
5. Yim Y, Kikkawa Y, Tanowaitz H, Wittner M. Fatal strongyloidiasis in Hodgkin's disease after immunosuppressive therapy. J Trop Med Hyg 1970;73:245–249.
6. Sato Y, Shiroma Y. Concurrent infections with *strongyloides* and T-cell leukemia virus and their possible effect on immune response of host. Clin Immunol Immunopathol 1989;52:214–24.
7. Nakada K, Yamaguchi K, Furugen S, Nakasone T, Nakasone K, Oshiro Y, et al. Monoclonal integration of HTLV-I proviral DNA in patients with strongyloidiasis. Int J Cancer 1987;40:145–8.
8. Potter A, Stephens D, De Keulenaer B. *Strongyloides* hyperinfection: a case for awareness. Ann Trop Med Parasitol 2003;97: 855–60.
9. Lemos LB, Qu Z, Laucirica R. Hyperinfection syndrome in strongyloidiasis: report of two cases. Ann Diagn Pathol 2003;7: 87–94.
10. Reiman S, Fisher R, Dodds C, Trinh C, Laucirica R, Whigham CJ. Mesenteric arteriographic findings in a patient with *Strongyloides stercoralis* hyperinfection. J Vasc Interv Radiol 2002;13: 635–8.
11. Setoyama M, Fukumaru S, Takasaki T, Yoshida H, Kanzaki T. SLE with death from acute massive pulmonary hemorrhage caused by disseminated strongyloidiasis. Scand J Rheumatol.1997;26: 389–91.
12. Finkielman JD, Grinberg AR, Paz LA, Plana JL, Benchetrit GA, Nicastro MA, et al. Case report: reactive hemophagocytic syndrome associated with disseminated strongyloidiasis. Am J Med Sci 1996;312:37–9.
13. Livneh A, Coman EA, Cho SH, Lipstein-Kresch E. *Strongyloides stercoralis* hyperinfection mimicking systemic lupus erythematosus flare. Arthritis Rheum 1988;31:930–1.
14. Wachter RM, Burke AM, MacGregor RR. *Strongyloides stercoralis* hyperinfection masquerading as cerebral vasculitis. Arch Neurol 1984;41:1213–6.
15. Webster E, Ballinger WE Jr, Panush RS. A case of a patient with deteriorating multisystem disease. Ann Allergy 1984;52:399–400; 423–7.
16. Berger R, Kraman S, Paciotti M. Pulmonary strongyloidiasis complicating therapy with corticosteroid. Report of a case with secondary bacterial infections. Am J Trop Hyg 1980;29:31–4.
17. Rivera E, Maldonado N, Velez-Garcia E, Grillo AJ, Malaret G. Hyperinfection syndrome with *Strongyloides stercoralis*. Ann Intern Med 1970;72:199–204.
18. Tada H, Masamune K, Takeda Y. A case of malnutrition associated with strongyloidiasis. Gastroenterol Endosc 1981;23: 1571–7.
19. Braley SL, Diens DE, Brewer NS. Disseminated *Strongyloides stercoralis* in an immunosuppressed host. Mayo Clin Proc 1987;53: 332–5.
20. Igra-Siegman Y, Kapila R, Sen P, Kaminski ZC, Louria DB. Syndrome of hyperinfection with *Strongyloides stercoralis*. Rev Infect Dis 1981;3:397–407.
21. Mori S, Konishi T, Matsuoka K, Deguchi M, Ohta M, Mizuno O, et al. Strongyloidiasis associated with nephrotic syndrome. Intern Med 1998;37:606–10.
22. Marti H, Haji HJ, Savioli L, Chwaya HM, Mgeni AF, Ameir JS, et al. A comparative trial of a single-dose ivermectin versus three days of albendazole for treatment of *Strongyloides stercoralis* and other soil-transmitted helminth infections in children. Am J Trop Med Hyg 1996;55:477–81.
23. Naquira C, Jimenez G, Guerra JG, Bernal R, Nalin DR, Neu D, et al. Ivermectin for human strongyloidiasis and other intestinal helminths. Am J Trop Med Hyg 1989;40:304–9.

Intracellular IL-1α-binding proteins contribute to biological functions of endogenous IL-1α in systemic sclerosis fibroblasts

Yasushi Kawaguchi*, Emi Nishimagi, Akiko Tochimoto, Manabu Kawamoto, Yasuhiro Katsumata, Makoto Soejima, Tokiko Kanno, Naoyuki Kamatani, and Masako Hara

Institute of Rheumatology, Tokyo Women's Medical University, 10-22 Kawada-cho, Shinjuku-ku, Tokyo 162-0054, Japan

Edited by Charles A. Dinarello, University of Colorado Health Sciences Center, Denver, CO, and approved August 8, 2006 (received for review May 2, 2006)

The aberrant production of precursor IL-1α (pre-IL-1α) in skin fibroblasts that are derived from systemic sclerosis (SSc) is associated with the induction of IL-6 and procollagen, which contributes to the fibrosis of SSc. However, little is understood about how intracellular pre-IL-1α regulates the expression of the other molecules in fibroblasts. We report here that pre-IL-1α can form a complex with IL-1α-binding proteins that is translocated into the nuclei of fibroblasts. Immunoprecipitation that used anti-human IL-1α Ab and ^{35}S-labeled nuclear extracts of fibroblasts showed three specific bands (≈31, 35, and 65 kDa). The 31-kDa molecule was identified as pre-IL-1α, and the 35- and 65-kDa molecules might be pre-IL-1α-binding proteins. A partial sequencing for the 10 aa from the N-terminals of the molecules showed 100% homology for HAX-1 (HS1-associated protein X-1) and IL-1 receptor type II (IL-1RII). Suppression of the genes of HAX-1 or IL-1RII induced the inhibitory effects of IL-1 signal transduction, including production of IL-6 and procollagen, by fibroblasts. In particular, pre-IL-1α was not translocated into the nucleus by an inhibition of HAX-1. These findings reveal that nuclear localization of pre-IL-1α depends on the binding to HAX-1 and that biological activities might be elicited by the binding to both HAX-1 and IL-1RII in SSc fibroblasts.

IL-1 receptor type II | HS1-associated protein X-1 | fibrosis | collagen | IL-6

Systemic sclerosis (SSc) is a connective tissue disease of unknown etiology that is characterized by the fibrosis of systemic organs (1). Because skin thickening manifests in most patients, researchers have analyzed the molecular and biological functions of lesional skin fibroblasts that are derived from SSc patients (2). In previous reports we demonstrated that SSc fibroblasts expressed IL-1α mRNA constitutively and that aberrant production of precursor IL-1α (pre-IL-1α) contributed to skin fibrosis in SSc (3–5). IL-1α is a multifunctional molecule that is involved in a variety of inflammatory disorders, including sepsis, arthritis, myositis, psoriasis, periodontitis, and Alzheimer's disease (6). Pre-IL-1α is synthesized as a result of the transcription and translation of the *IL1A* gene. Under some circumstances, pre-IL-1α (31 kDa) is proteolytically cleaved to yield a mature form of IL-1α (17 kDa) (7). Because the N-terminal propiece of pre-IL-1α (NTP-IL-1α) contains a nuclear localization sequence (NLS), pre-IL-1α can be translocated into the nucleus, whereas mature IL-1α can be released from cells (8).

This pathway is complicated, however. The signal transduction of IL-1α is initiated by the binding of IL-1α (precursor or mature form) to cell-surface receptors on various cells (IL-1 receptor type I and IL-1 receptor accessory protein) (9, 10). The intracellular accumulation of pre-IL-1α in skin fibroblasts suggests an alternative pathway. Only a few studies, including ours, have reported the biological effects of intracellular IL-1α in fibroblasts and endothelial cells (11–15). Although the precise pathway of signal transduction was not determined in those studies, the authors speculated that intracellular pre-IL-1α might exhibit a biological function directly and that the pathway of signal transduction might be distinct from the pathway that was mediated by binding the specific receptors. Our previous study (5) revealed that intracellular pre-IL-1α directly influenced the phenotype of SSc fibroblasts. These observations prompted us to explore the mechanism whereby intracellular pre-IL-1α exhibits its biological functions through the alternative pathway. In the present study we investigate the molecules that bind to pre-IL-1α in human fibroblasts and the effects of the IL-1α-binding proteins on nuclear localization and biological functions of IL-1α.

Results

Localization of Intracellular IL-1α in SSc Fibroblasts. Although we previously demonstrated the nuclear localization of pre-IL-1α in SSc fibroblasts, we performed immunohistochemistry on five lines of SSc fibroblasts and three lines of normal fibroblasts. We visualized the signals of intracellular IL-1α in all five SSc fibroblast lines and did not detect them in the three normal fibroblast lines. A representative result of Cy3 staining is shown in Fig. 1. The specific signals were mostly distributed in the nucleus, consistent with our previous results (5).

Immunoprecipitation (IP). To detect candidates of intracellular IL-1α-binding proteins, we used cell lysates of SSc fibroblasts and anti-IL-1α Ab to perform IP. As shown in Fig. 2, autoradiography indicated that the lengths of the specific bands were ≈31, 35, and 65 kDa. Columns 2 and 3 show representative data from IP that use cell lysates of SSc fibroblasts with anti-IL-1α Ab under a nonreducing and a reducing condition, respectively, and column 1 shows data that use cell lysates of SSc fibroblasts with rabbit IgG under a reducing condition. The 31-kDa band corresponded to the predicted pre-IL-1α in fibroblasts. Because the 35- and 65-kDa bands were also candidates of the intracellular IL-1α-binding proteins, we used a protein sequencer to partially analyze the N-terminals of these molecules. The 35-kDa molecule was homologous to HAX-1 (HS1-associated protein X-1; amino acid sequence MSLFDLFRGF), and the 65-kDa molecule was homologous to IL-1 receptor type II (IL-1RII; amino acid sequence FTLQPAAHTG). We observed no specific bands below the 30-kDa molecule (data not shown). Thus, we con-

Author contributions: Y. Kawaguchi, E.N., A.T., Y. Katsumata, M.S., T.K., N.K., and M.H. designed research; Y. Kawaguchi, E.N., A.T., and M.K. performed research; Y. Kawaguchi, E.N., A.T., M.K., Y. Katsumata, M.S., T.K., N.K., and M.H. analyzed data; and Y. Kawaguchi wrote the paper.

The authors declare no conflict of interest.

This paper was submitted directly (Track II) to the PNAS office.

Abbreviations: Ct, threshold cycle; HAX-1, HS1-associated protein X-1; icIL-1RA, intracellular IL-1 receptor antagonist; IL-1RII, IL-1 receptor type II; IP, immunoprecipitation; NTP-IL-1α, N-terminal propiece of pre-IL-1α; pre-IL-1α, precursor IL-1α; SSc, systemic sclerosis.

*To whom correspondence should be addressed. E-mail: y-kawa@ior.twmu.ac.jp.

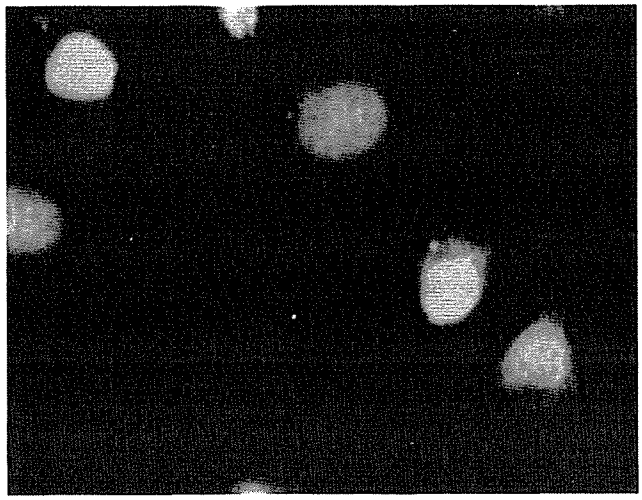

Fig. 1. Nuclear localization of IL-1α in SSc fibroblasts. SSc fibroblasts were cultured in plates on a four-chamber slide. Cells were fixed with 2% paraformaldehyde plus 0.1% Triton X-100. The primary Ab was monoclonal anti-human IL-1α Ab, which detected pre-IL-1α and mature IL-1α after incubation with Cy3-conjugated anti-mouse IgG Ab. A representative result in SSc fibroblasts was obtained with fluorescence microscopy.

cluded that intracellular IL-1α was almost pre-IL-1α (31 kDa) in SSc fibroblasts, consistent with our previous studies (3–5).

Expression of IL-1RII and HAX-1 in Fibroblasts. To confirm the expression of IL-1RII and HAX-1 in SSc and normal fibroblasts, we used RT-PCR to analyze the expression of mRNA. The cDNA that was derived from five fibroblast lines of patients with SSc contained mRNA of both IL-1RII and HAX-1, but three normal fibroblast lines contained the HAX-1 mRNA alone (Table 1). Western blotting indicated that HAX-1 was expressed in SSc and normal fibroblasts, but we detected IL-1RII in SSc fibroblasts alone (Fig. 3). Immunocytochemical studies revealed different distributions of HAX-1 and IL-1RII between SSc and normal fibroblasts (Fig. 4). HAX-1 was localized in the nuclei and cytosol of SSc fibroblasts but in only the cytosol of normal fibroblasts. IL-1RII was localized in the nuclei and cytosol of

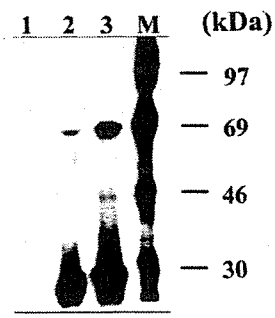

Fig. 2. Pre-IL-1α-binding proteins were detected by IP. Fibroblasts from SSc were cultured by using [^{35}S]methionine/cystein for 16 h. After a pulse, cells were harvested and sonicated to extract nuclear and cytosolic proteins. IP was performed with cell lysates and anti-human IL-1α Ab or control rabbit IgG combined with protein G-Sepharose. Immunoprecipitates were fractionated by 10% SDS/PAGE, and radiolabeled polypeptides were visualized by autoradiography. Column 1, lysate reacted with rabbit IgG fractionated under a reducing condition; column 2, lysate reacted with anti IL-1α Ab fractionated under a nonreducing condition; column 3, lysate reacted with anti IL-1α Ab fractionated under a reducing condition; column M, molecular marker.

Table 1. Expression of IL-1RII and HAX-1 mRNA in cultured fibroblasts

Subjects	IL-1RII	HAX-1
SSc		
1	17	4.3
2	15	5.2
3	29	42
4	31	26
5	25	18
HC		
1	<0.01	20
2	0.02	21
3	<0.01	48

Total RNA was extracted from cultured fibroblasts derived from five patients with SSc and three healthy controls (HC). Real-time RT-PCR was performed by using an ABI 7900HT and FAM-labeled TaqMan gene expression assay kit. GAPDH mRNA expression was used as an endogenous control.

SSc fibroblasts, and no fluorescent signal was detected in normal fibroblasts.

Binding Capacities of IL-1RII to Pre-IL-1α in Fibroblasts. To investigate the binding capacities of IL-1RII to pre-IL-1α in fibroblasts, we produced murine fibroblasts that were transfected with human pre-IL-1α, human IL-1α, or human NTP-IL-1α, which were cotransfected with human IL-1RII. We detected human IL-1RII, which was expressed by the pcDNA3 vector, in murine fibroblasts by anti-IL-1RII Ab (Fig. 5, second row). Because three forms of human IL-1α were expressed as V5-tagged proteins in murine fibroblasts, these proteins were detected by anti-V5 Ab (Fig. 5, third row). Finally, after cell lysates from murine fibroblasts were immunoprecipitated with anti-IL-RII Ab, human IL-1α and human pre-IL-1α were detected by Western blotting with anti-V5 Ab (Fig. 5). These results indicate that intracellular IL-1RII binds to pre-IL-1α and mature IL-1α via the amino acid sequence from 113 to 271 aa.

To confirm the interaction of IL-1α with IL-1RII and HAX-1, we fused cDNA that encodes three kinds of IL-1α to the λ repressor protein (λcI) of pBT plasmid and fused each target gene of IL-1RII and HAX-1 to the N-terminal domain of RNA polymerase of pTRG plasmid. We grew double transforming cells of pre-IL-1α with IL-1RII or HAX-1 in selection LB plates and had a β-galactosidase activity (Fig. 6). The cells transformed with NTP-IL-1α were positive only when cotransformed with HAX-1, and the cells transformed with IL-1α were positive only when cotransformed with IL-1RII. Previously, HAX-1 was reported to be associated with three sites of NTP-IL-1α (16). By considering all this evidence, we present a schematic of putative pre-IL-1α complex in Fig. 7.

Functional Roles of IL-1RII and HAX-1 in the Signal Transduction of Pre-IL-1α. To further investigate the roles of IL-1RII and HAX-1 as a pre-IL-1α-binding protein, we produced SSc fibroblasts that deplete IL-1RII or HAX-1 by means of RNA interference.

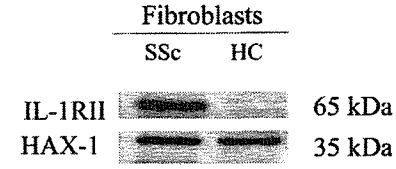

Fig. 3. Western blot analysis of IL-1RII and HAX-1 in fibroblasts. Cell lysates were prepared from fibroblasts derived from systemic sclerosis (SSc) and a healthy donor (HC).

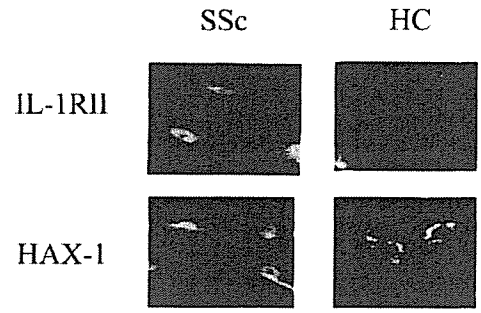

Fig. 4. Cellular distribution of IL-1RII and HAX-1 by immunofluorescence staining. Fibroblasts were fixed by 2% paraformaldehyde plus 0.1% Triton X-100 and then reacted with anti-IL-1RII or anti-HAX-1 Ab. After they were treated with FITC-conjugated anti-mouse IgG, a fluorescence image was obtained.

IL-1RII and HAX-1 proteins were suppressed in all five lines of SSc fibroblasts transfected with a small siRNA-expressing vector. A representative result of Western blotting is shown in Fig. 8. We used five lines of SSc fibroblasts to conduct the experiments, and then we scanned each band on x-ray films on a scanning densitometer. We measured the intensity of each molecule by subtracting the intensity of background from that of the band. The mean ratio of specific/random siRNA was 0.06 in IL-1RII and 0.21 in HAX-1. An inhibition of IL-1RII did not affect the nuclear localization of pre-IL-1α, but inhibiting HAX-1 caused the nuclear staining of pre-IL-1α in SSc fibroblasts to disappear (Fig. 9). We used five different lines of SSc fibroblasts to confirm this result. We previously demonstrated that aberrant production of pre-IL-1α in the nucleus contributed to IL-6 and procollagen type I production in SSc fibroblasts. To explore the effects of IL-1RII and HAX-1 on IL-6 and procollagen type I production in SSc fibroblasts, we suppressed the production of both IL-6 and procollagen type I by the knockdown of IL-1RII and HAX-1 (Fig. 10 *A* and *B*). The results indicate the mean of triplicate experiments that use five SSc fibroblasts and three normal fibroblasts.

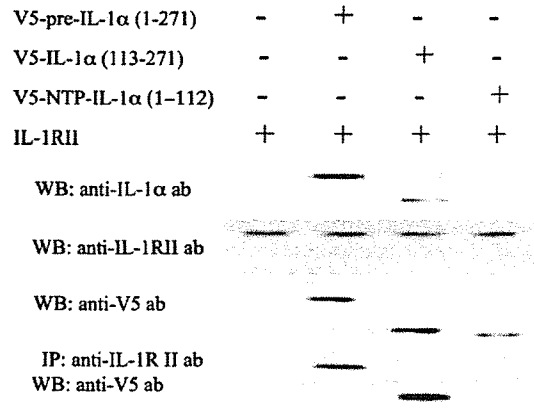

Fig. 5. A binding assay of pre-IL-1α and IL-1RII was performed with murine fibroblasts (NIH 3T3) transfected with human IL-1α and IL-1RII. The cDNA of human IL-1α (amino acids 113–271), pre-IL-1α (amino acids 1–271), and NTP-IL-1α (amino acids 1–112) were subcloned into the pcDNA4-V5 vector. The cDNA of human IL-1RII was subcloned into the pcDNA3 vector. NIH 3T3 cells were transfected with one of three kinds of pcDNA4-V5 and pcDNA3, as indicated above the panels. Cell lysates were extracted from each transfectant by sonication. The upper three panels indicate the results of Western blotting (WB) with anti-IL-1α Ab, anti-IL-1RII Ab, and anti-V5 Ab. The lowest panel indicates the results of WB with anti-V5 Ab after IP that used anti-IL-1RII Ab.

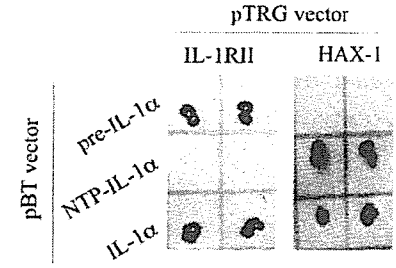

Fig. 6. A bacterial two-hybrid system was performed to confirm the interaction between pre-IL-1α and its binding proteins (IL-1RII and HAX-1). The IL-1α proteins were fused to the bacteriophage λ repressor protein by using pBT plasmid, and the target proteins (IL-1RII and HAX-1) were fused to the N-terminal domain of RNA polymerase by using pTRG plasmid. The suitable *E. coli* was transformed by the two plasmids, and LB agar plates, including tetracycline, chloramphenicol, kanamycin, and X-gal, were used to select positive clones.

Discussion

The results of the present study provide solid evidence that intracellular pre-IL-1α consists of a protein complex with IL-1RII and HAX-1 and that the formation of this complex is indispensable for pre-IL-1α-induced biological functions (IL-6 production and procollagen type I synthesis by fibroblasts). Our previous findings indicated that nuclear localization of pre-IL-1α plays a crucial role in the fibrogenic phenotype of skin fibroblasts derived from patients with SSc (3–5). The present study demonstrates the importance of the pre-IL-1α complex for the fibrogenic phenotype of SSc fibroblasts.

Early research indicated that IL-1α or pre-IL-1α is secreted from cells and exhibited an inflammatory response and immunity through the specific IL-1 receptors on the surface of targeted cells. However, intracellular pre-IL-1α has been shown to stimulate proliferation of renal fibroblasts (11) and to regulate the migration and the life span of endothelial cells (12), independent of secretion and cell-surface IL-1 receptors. Some researchers suggested that the nuclear localization sequence in the NTP-IL-1α molecule might be essential for the biological activity of intracellular IL-1α (11, 12). Recently, Buryskova *et al.* (13) observed that intracellular pre-IL-1α functionally activated transcription, interacting with histone acetyltransferase complexes. Werman *et al.* (14) reported that intracellular IL-1α is

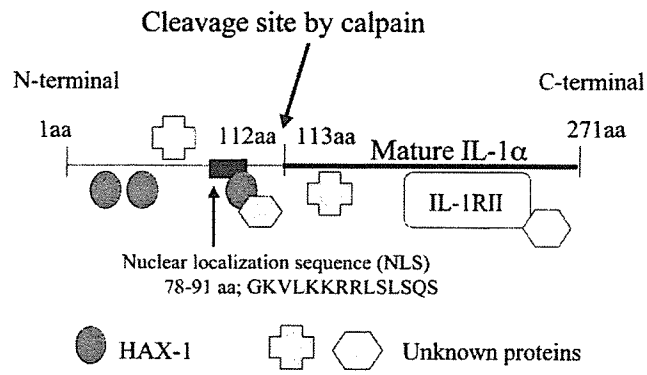

Fig. 7. A putative structural component of the pre-IL-1α complex in fibroblasts. IL-1RII binds to the C-terminal domain of pre-IL-1α, and HAX-1 binds to the N-terminal domain in fibroblasts. However, unknown proteins, aside from these two, may bind to pre-IL-1α and unknown proteins may directly bind to IL-1RII or HAX-1. The component proteins within the pre-IL-1α complex may possess the DNA- or RNA-binding motif, which may allow the pre-IL-1α complex to modulate the fibrosis and inflammation.